**Progress In Oceanography**
January-February 2010, Volume 84, Issues 1-2, Pages 69-84
http://dx.doi.org/10.1016/j.pocean.2009.09.008




# Bridging the gap from ocean models to population dynamics of large marine predators: A model of mid-trophic functional groups

Patrick Lehodey[a, *], Raghu Murtugudde[b] and Inna Senina[a]

[a] MEMMS (Marine Ecosystems Modeling and Monitoring by Satellites), CLS, Space Oceanography Division, 8-10 rue Hermes, 31520 Ramonville, France
[b] ESSIC, Earth Science System Interdisciplinary Center, University of Maryland, USA

* Corresponding author : Patrick Lehodey, Tel.: +33 561 393 770; fax: +33 561 393 782, email address : PLehodey@cls.fr

**Abstract:**

The modeling of mid-trophic organisms of the pelagic ecosystem is a critical step in linking the coupled physical–biogeochemical models to population dynamics of large pelagic predators. Here, we provide an example of a modeling approach with definitions of several pelagic mid-trophic functional groups. This application includes six different groups characterized by their vertical behavior, i.e., occurrence of diel migration between epipelagic, mesopelagic and bathypelagic layers. Parameterization of the dynamics of these components is based on a temperature-linked time development relationship. Estimated parameters of this relationship are close to those predicted by a model based on a theoretical description of the allocation of metabolic energy at the cellular level, and that predicts a species metabolic rate in terms of its body mass and temperature. Then, a simple energy transfer from primary production is used, justified by the existence of constant slopes in log–log biomass size spectrum relationships. Recruitment, ageing, mortality and passive transport with horizontal currents, taking into account vertical behavior of organisms, are modeled by a system of advection–diffusion-reaction equations. Temperature and currents averaged in each vertical layer are provided independently by an Ocean General Circulation Model and used to drive the mid-trophic level (MTL) model. Simulation outputs are presented for the tropical Pacific Ocean to illustrate how different temperature and oceanic circulation conditions result in spatial and temporal lags between regions of high primary production and regions of aggregation of mid-trophic biomass. Predicted biomasses are compared against available data. Data requirements to evaluate outputs of these types of models are discussed, as well as the prospects that they offer both for ecosystem models of lower and upper trophic levels.

# 1. Introduction

The level of information, both in terms of understanding and observations, for the physical and biogeochemical components of the pelagic ecosystem is now sufficient to make realistic basin scale simulations of ocean physics and lower trophic (phytoplankton) level biology. On the other hand, the information is still very limited for the intermediate or mid-trophic levels (micronekton). Yet, the modeling of these components is quintessential for understanding the dynamics of their predators that are most often heavily exploited species. Pressing management issues require rapid developments in understanding and prediction of the changes occurring in these populations under the pressures of both fishing and climate change. Thus, it is a primary condition to develop a new generation of models for the study and management of these exploited marine resources whose exploitation attracts increasing concerns on their sustainability or even a risk of extinction in some cases.

Given these pressing issues, the modeling approach certainly requires realism and pragmatism, especially if we use “ecosystem” in its whole sense that is including both the physical environment and the set of all living organisms and their interactions in space and time, with each other and with their environment. There is an obvious huge gap between the recent achievements in physical oceanography, with the development of ocean general circulation models (OGCMs), and our capacity to model the incredible complexity of the marine life. Though less advanced in understanding and representation of underlying mechanisms, the new generation of biogeochemical models (BGCM) appears also mature enough to capture the global features (spatio-temporal, seasonnal-to-interannual and multi-decadal variability) of the components of the carbon cycle. Of course, there is still a vast field of research for including increasing complexity of processes, in particular over the continental slopes, shelf-breaks, and coastal areas, but at least there is a simplified and coherent vision of these biogeochemical components, and the coupling between OGCM and BGCM (OGCBM) is now a common practice. In addition, for both types of models, there exist synoptic (satellite-derived) and *in-situ* observations allowing model evaluation and data assimilation.

The situation is remarkably different as soon as we move up a step in this great ecosystem picture, i.e. for zooplankton and more particularly the mid-trophic levels that constitute forage organisms of predator species; the latter being frequently exploited marine resources. The challenge proposed here is to model these components of the marine ecosystem despite the very limited knowledge and observation available, thus using an approach as simple as possible, but that can be coupled nonetheless, to the other components (OGCBM) without loosing the benefit of the better insights and detailed modeling possibility they offer. This means that the new modelled components have to be spatially-explicit and at least constrained by their bio-physical environment predicted by the OGCBM, if not fully coupled to investigate potential biological feedbacks.

Given the diversity of species and interactions in the food web structure, the approaches for modeling ecosystem ecology rely mainly on the energetic view as stated by Lindeman (1942), describing the ecosystem as a flow of energy through a network from the first trophic level (primary producers) to the consumers groups. The question is how to define these groups. In its simplest expression, it would be a chain of discrete trophic levels, as in a trophic pyramid. The concept then can be extended to a larger number of groups producing an increasingly complex network with potential interactions between one group and all the others, and requiring the introduction of a continuous representation of trophic levels.

The approach of trophic flow models has been proposed and used for investigating different marine ecosystems (Christensen and Pauly 1992) but it becomes limited by the extensive number of parameters exponentially increasing with the number of groups defined to represent the network. The parameterization of the trophic network in such models becomes an unrealistic static view when considering the plasticity of organisms and their aptitude to switch from one prey (or group of prey) to another. Besides, most of oceanic large predators are opportunistic feeders with a very large spectrum of prey species. In addition, the definition of groups by trophic levels may be problematic since organisms can occupy many different trophic levels over their life.

A second approach is then to consider the size spectrum in the ecosystem. The size was effectively identified as a fundamental criterion that structures the ecosystem, especially the marine ecosystem. The size of an organism largely determines its function in the ecosystem: it controls the diet based (roughly) on prey-predator size relationships; there is an obvious size-abundance relationship, the smaller organisms being the most abundant (Elton, 1927); and finally metabolism and turn-over also appear linked to it. These latter relationships have been investigated for long and seen in multiple empirical observations. Kleiber (1932) was the first to provide a surprising result by showing that an animal's metabolic rate is proportional to its body mass raised to the power of ¾. Since then, scaling laws based on exponents in which the denominator is a multiple of four have been proposed in various ways. Empirical data also suggest allometric relationships between abundance per unit area and body size (or weight) both in terrestrial and marine systems (e.g., Sheldon et al. 1972; Kerr 1974; Enquist et al. 1998; Belgrano et al 2002), or similarly between weight of organisms and the growth rate of their population (Fenchel 1974, Savage et al. 2004). It follows from these findings that abundance at a given size (weight) or "size window" is constrained by rates of energy supply, thus leading to macroecological properties. Therefore, abundance or biomass-body size (weight) relationships have been used to describe the energy flow in biomass size spectrum in different ecosystems which interestingly showed similar slopes in log-log relationships (Dickie 1976, Boudreau and Dickie 1992).

Underlying mechanisms that can explain these scaling laws are obviously of critical significance for ecological modeling. Platt and Denman (1978) proposed a first attempt to understand the size structure of pelagic ecosystems under energetic balances. They demonstrated that "*the trophic structure of an ecosystem is controlled in some way by the magnitudes of various physiological rates of the component organisms*" (Platt 1985), thus establishing the allometric basis that structures the marine ecosystems. More recently, a theory known as the Metabolic Theory of Ecology (MTE) has been proposed by Brown et al. (2004) to describe how the metabolic rate of individual organisms varies with body mass and temperature. Another approach proposed previously by Kooijman (1986) was based on a model of dynamics energy budget (DEB). Though based on similar principles (e.g., the van Hoff-Arrhenius equation), the approaches are different and debated (Van der Meer, 2006), and will require much work and experimentation before providing the kind of unifying conceptual frameworks needed for modeling the ecosystem based on molecular principles.

Nevertheless, scaling laws like allometric relationships are now sufficiently well established to be used as a practical modeling approach especially since critical issues like climate change or management of (over) exploited marine species require the rapid development (e.g., in the coming 5-10 years) of "Minimum Realistic Models" (MRM) as defined by Butterworth and Plaganyi (2004), i.e. "*with the underlying concept to restrict the model developed to those species most likely to have important interactions with the species of interest*".

In this paper, one pathway is presented as an alternative to the size-spectrum approach that combines energetic and functional approaches, to model the mid-trophic level organisms of marine ecosystems. Instead of describing the full size-spectrum of the marine ecosystem, we propose to model several functional groups for a given size or weight window, corresponding to the biomass of forage organisms of large oceanic predators, i.e. roughly the micronekton. Rather than considering size, this approach is based on the temperature-linked development time of the organisms and the turnover of their multi-species population functional groups. The bio-physical forcing provided by one OGCBM is used to produce a simulation of the mid-trophic functional components. Then the interest of representing these new functional groups as a link for investigating and modeling the dynamics of fish populations is discussed.

## 2. Modelling approach

### 2.1. Conceptual model of the mid-trophic functional groups

Oceanic micronekton includes a myriad of species providing forage for larger predators. They can be roughly characterized by a size spectrum in the range of 2~20 cm dominated by crustaceans, fish, and cephalopods. Gelatinous organisms like jellyfish are also likely an underestimated important component of micronekton in the functioning of the system but apparently have a limited number of predators. One distinctive characteristic of most of these organisms is to perform diel vertical migrations, moving between deep layers during the day to the surface layer at night. This evolutionary adaptation likely decreases the predation pressure during the day in the upper layer though predators also have adapted their behavior under the same constraints, i.e. finding food and avoiding bigger predators. But the essential result is that the flow of energy generated by autotrophic organisms in the euphotic layer is transferred to the deeper meso- and bathy-pelagic layers through these daily migrations. Acoustic and micronekton sampling studies indicate that most of the micronekton biomass occupies the meso- and bathy-pelagic layer. Therefore, according to Legand et al. (1972), and Grandperrin (1975), about 90% of the biomass of macroplankton and micronekton in the tropical Pacific Ocean is typically concentrated in the 0-500 m upper layer during the night and 50% in the 0-100m layer, however only 10% remains in the first 200 m during the day. Similarly, Hidaka et al. (2003) found a factor 10 between day and night biomass of micronekton in the upper 200m of the western tropical Pacific Ocean. Predators of these mid-trophic organisms have evolved to prey upon these species, i.e., either they chase the prey species migrating in the layer they inhabit, or they make temporary excursions in the layers where these species remain. Through evolution, the predators have thus developed sensory, morphological and physiological adaptations allowing them to exploit cold, dark and sometimes oxygen depleted deep layers. Hence, vertical movements appear to be a key process in structuring the ocean ecosystem, and therefore an essential mechanism that has to be accounted for when designing a functional view of the system.

Following this idea, and based on existing knowledge (cf. a review in appendix A), a simple conceptual model of the mid-trophic level components can be proposed with six functional groups in three vertical layers: epipelagic, mesopelagic and bathypelagic (Fig. 1). The pelagic micronekton is divided into epipelagic, mesopelagic and bathypelagic groups, the last two groups subdivided into vertically migrant and non-migrant species. Since light intensity is likely a major factor that controls diel vertical migrations of meso- and bathypelagic organisms, the euphotic depth is a logical and convenient way to define the vertical boundaries of the three

layers. Preliminary examinations of predicted euphotic depths from biogeochemical models indicate that using the euphotic depth as the boundary for the epipelagic layer and defining the boundary between meso- and bathypelagic layers by three times the euphotic depth would produce values similar to those defined from biological observations, e.g., between 50 and 150 m for epipelagic and 150 and 450 m for mesopelagic layers in the eastern and western tropical Pacific Ocean respectively.

### 2.2. Spatio-temporal dynamics of functional groups

Here, micronekton functional groups are considered as single populations composed of different species, and then modeled using the same equations as for single population model (see previous references in Lehodey et al. 1998, Lehodey 2001), with continuous mortality and recruitment (e.g., Ricker 1975). Instead of having different age classes (cohorts) of the same species, there are different age classes of many different species, the mathematical solution being the same (Allen, 1971).

The concept of this model dynamics was illustrated as follows (Lehodey, 2004a): "*at any time, anywhere in the ocean, there is a mixing of all kinds of eggs, cells, etc… that are the germs of the future organisms of the pelagic food web. In some places and at some times, the input of nutrients into the euphotic zone allows an almost immediate development of phytoplankton (primary production P) that is the input source into the forage population model (F). This new production allows the development of a new "cohort" of organisms, i.e., true zooplankton like copepods as well as all larvae of fish and other larger organisms (meroplankton). The organisms having a longer lifespan and a larger growth potential (larvae and juvenile of fish, squids, shrimps, etc.) feed at the expense of the organisms with a shorter lifespan and a lower growth potential (phytoplankton, zooplankton). As the water masses are maturing, they are advected with these organisms (but a part of them can also diffuse away due to the diffusion of water and their own random movements) and the currents create fronts of convergence where forage is aggregated. Of course these dynamics occur as a continuous process in time and space. Following this time-trophic continuum concept, the species [for a given cohort] should disappear selectively in the order of their trophic level related to their time of development".* At the time ($t_r$) they are entering (~ recruited in) the forage population *F* (biomass), the survival organisms – the amount of which is linked to the energy efficiency coefficient *E* – provide the forage production (*F'*).

In this approach there is no size structure in functional groups but accumulation of biomass (after a given recruitment time $t_r$) through an energy efficiency coefficient *E* with primary production as the source. However, these functional groups can be considered as body-size "windows" of the full size spectrum of the marine system. Given the lack of detailed information concerning the consumption rates and the links between zooplankton and micronekton groups, it was in fact an easy and feasible way at this stage to implement ecological transfer from primary production to micronekton groups (see appendix B). This representation appears sufficient for developing new modeling approaches and applications to population dynamics of exploited species (see discussion).

The spatial dynamics is considered and described with an advection-diffusion equation using horizontal currents for the advective terms and a diffusion coefficient ($\rho$=10 000 $m^2s^{-1}$) incorporating both diffusion of water and random movement of organisms. During the time that a mid-trophic functional group is occupying its day or night layer, it is transported by the currents averaged through corresponding layers. The time spent in one or the other layer is calculated from the day length equation as a function of the latitude and the Julian day (see appendix C).

### 2.3. Parameterization of the turnover of the functional groups

The turnover of mid-trophic functional groups is controlled by the parameter $\lambda$ (mortality coefficient) and the parameter $t_r$ that is the minimum age to be recruited in the mid-trophic functional population. The sum $t_r+1/\lambda$ is equivalent to the "mean age" of the population, and the maximum lifespan defined as the time necessary to see the population reduced to a determined level (e.g., $x$ = 1% or 5%) is $t_{max} = -1/\lambda \text{ Ln}(x) + t_r$ (Lehodey 2001). The turnover of a population is usually defined as the generation time or the average age at maturity $t_m$ of the individuals in the population, hence it is useful to search for a relation between age at maturity and the mean age of population that could help in the parameterization of $\lambda$. Indeed, age at maturity and lifespan are important criteria in population dynamics and it has been empirically demonstrated in a study by Froese & Binohlan (2000) that they are both linked following a log-log linear relationship (eq. 1).

$$\log(t_{\max}) = 0.5496 + 0.957 \log(t_m) \qquad \text{(Equation 1)}$$

By substituting $t_{max}$ by its definition above, we obtain equation (2):

$$t_m^{0.957} = -\frac{\ln(x)}{10^{0.5496} \cdot \lambda} + \frac{1}{10^{0.5496}} \cdot t_r \qquad \text{(Equation 2)}$$

Given the range of standard error of the original regression (Froese and Binohlan 2000), and taking $x$ = 0.05, equation (2) can be simplified into equation (3):

$$t_m = 1/\lambda + 1/3\ t_r \qquad \text{(Equation 3)}$$

As useful as this relationship can be, it would be more satisfying to deduce a formal relationship between mortality $\lambda$ and $t_m$ from a theoretical basis. The dynamic energy budget (Kooijman, 1986) or the Metabolic Theory of Ecology (Brown et al., 2004) may offer such a theoretical framework. At the individual level, population turnover is linked to biological rates of individual organisms and then relies on the metabolic rates at which these organisms use and transform energy and materials (e.g., Platt 1985; Savage et al. 2004). These rates obey the thermodynamic laws, i.e., the physical and chemical principles that govern the transformation of energy and materials, and while the metabolism is linked to the size of organisms, the time needed to reach a given size (weight) is constrained by the ambient temperature.

Gillooly et al. (2002), following the work of West et al. (1997, 2001), describe the allocation of metabolic energy at the cellular level, having developed a model that predicts a linear relationship between the natural logarithm of a mass-corrected development time ($t/m^{1/4}$) and the ambient temperature at which the development stage occurs ($T_c$ in $^oC$), or to be more precise, the term $T_c/(1+(T_c/273))$. They illustrated the capacity of the model to show how size and temperature affect embryonic development time of aquatic ectotherms (fish, amphibians, aquatic insects, and zooplankton) and birds, as well as the post-embryonic to maturity development time of zooplankton species. Their model predicts approximately universal straight line with the slope, $\alpha = -\bar{E}/k\ T_0^2$ with $\bar{E}$ the activation energy for metabolic reactions, $k$ the Boltzmann's constant and $T_0$ =273 K. Because both the slope and intercept depend on fundamental cellular properties, they do not vary significantly across taxa. With $\bar{E} = 0.6\ eV$ (an average of the observed range

0.2-1.2 eV), the model predicts α = -0.09 per $^{o}$C, while values obtained by regression from different data sets are in the range of -(0.11-0.14) (Gillooly et al. 2002).

Similarly, we have investigated the relationship between age at maturity of mid-trophic species and their ambient temperature. Unfortunately it is very difficult to obtain from the literature the three variables needed, i.e. the age at maturity $t_m$, the body mass at maturity $m$ and the ambient temperature $T_c$. We were able however to compile a dataset of $t_m$ and $T_c$ for mid-trophic species of the main taxa of ocean mid-trophic groups, i.e., crustaceans, fish and squid. Parameters were estimated from a log-linear regression (equation 4; Fig. 2) that gives a good fit to the data ($N_{obs}$ = 45; $R^2$ = 0.889).

$$\mathrm{Ln}(t_m) = 7.654 - 0.125\ (T_c / (1 + (T_c / 273)) \qquad \text{equation (4)}$$

To be fully comparable with the model proposed by Gillooly and co-authors, observations of time of development to age at maturity for these species (Fig. 2) should be also corrected relatively to the mass factor ($m^{1/4}$). Nevertheless, it is clear that these results suggest that Gillooly et al.'s model could be effectively extended to these other taxa, at least concerning the development time until the onset of maturity during which the energy is devoted to growth and somatic maintenance only. The slope (-0.125) and the intercept (7.654) that we obtained are in the range of what has been obtained with other datasets (Gillooly et al., 2002).

Finally, substituting $1/\lambda + 1/3\ t_r$ for $t_m$ into equation 4, we obtain a parameterization of $\lambda$ linked to the ambient temperature and $t_r$ (Fig. 2). The parameterization of $t_r$ itself would require a detailed study to compile a dataset of time of development, i.e., age, and ambient temperature for organisms to reach the minimum size of the modeled mid-trophic functional groups. Indeed, a relationship of temperature-linked time of development to reach a minimum weight would be more accurate. On the basis of a few observations from tuna diets, we have fixed to 1g the minimum weight of the mid-trophic groups, e.g., this is the average weight of pelagic crab megalopa that are eaten in large number by yellowfin tuna off eastern Australia (pers. comm. from J. Young, CSIRO). Marine organisms reach this minimum weight in much less than one month in warm waters (>28°C); a good example is given by tuna larvae that can reach 5 cm after only one month in the Pacific warm pool. In colder water (10-15°C) like in the upwelling systems of the Humboldt, California or Benguela, growth studies of anchovy, sardines and other Clupeidae suggest a value of $t_r$ above 2 months (Palomares et al., 1987). Finally in very cold water (<5°C) it may require more than 10 months to reach this minimum weight. In sub-antarctic waters (2-5°C) for example, pteropods, a small but important prey species of Pacific salmon, is adult after one year (Kobayashi 1974). Since there is no reason to have a different slope in the temperature relationship for $t_r$, we used $t_r = ¼\ t_m$ to match these very scarce observations (Fig. 2). This simple definition leads to a maximum value of 2109 days and 527 days for $1/\lambda$ and $t_r$ respectively at $T_c$ = 0°C and the same exponential coefficient (-0.125).

## 3. Model configuration and forcing data set

The model domain covers the Pacific Ocean with a grid extending from 65$^{o}$N to 50$^{o}$S at 1° x month resolution. To drive the intermediate trophic functional groups, we used physical and biogeochemical forcing data sets derived from a coupled physical-biogeochemical model.

The Ocean General Circulation Model (OGCM) is based on a reduced gravity, primitive equation, σ-coordinate model coupled to an advective atmospheric mixed layer model (Murtugudde et al. 1996). Numerous studies on tropical ocean variability, tropical-subtropical interactions, physical-biological feedbacks, and coupled ecosystem variability have been reported demonstrating the model's ability to capture the sub-seasonal to interannual variability of the dynamics and thermodynamics in the tropics (e.g., Chen et al., 1994, Murtugudde et al., 2002, Murtugudde et al., 2004).

A biogeochemical model has been fully coupled to the OGCM described above and tested in the three tropical oceans (Christian et al., 2002; Christian and Murtugudde, 2003; Wiggert et al., 2006). This model consists of nine components: two size-classes each (large and small) of phytoplankton, zooplankton and detritus, and three nutrient pools: ammonium, nitrate, and iron. The incorporation of iron into the ecosystem model is of vital importance for improving the prediction of the ecosystem response as iron has been identified as an important element controlling phytoplankton growth and biomass in large regions of the world's oceans (Coale et al. 1996; Martin, 1990; Martin et al., 1994). This model works well in reproducing ecosystem dynamics and biogeochemical fields at seasonal to interannual time scales (Wang et al. 2005; 2006a; 2006b), though the variability of primary production is underestimated, a tendency observed in all biogeochemical models (R. Feely 2005, personal communications). Figures 3 and 4 illustrate the ability of the model to capture the interannual and decadal variability in the primary production in the tropical, extra-tropical, and mid-latitude regions.

For simplicity in this first application, temperature and horizontal current variables were averaged in three vertical layers (see Appendix C for details), with fixed depths rather than based on variable euphotic depths: epipelagic (0-100m), mesopelagic (100-400m) and bathypelagic (400-1000m). The primary production was integrated trough 0-400m. The period of simulation spanned 1948-2004 period. A monthly climatology was created for all forcing variables as a monthly means computed over all years of simulation, and used for the spin-up to build up the biomass of the different functional groups and to reach equilibrium, i.e., practically, after a number of time steps ≥ ($t_{r\ max}$+1/$\lambda_{max}$). Though the simulation domain covered the full Pacific basin, we will focus our analysis on the tropical (30°N-30°S) region.

## 4. Results

### 4.1. Simulation outputs

The distribution in the epi-pelagic layer during the day is the most contrasted, due to higher temperature (faster turnover) and stronger environmental variability in this layer than in the deeper layers. On average, there is a latitudinal shift of maximum concentration that appears in the equatorial region on each side of the equator (Fig. 5). The maximum of biomass in the surface layer during the day occurs in the eastern Pacific in association with the coastal Peruvian upwelling and in the west in the shallow waters of the Papua New Guinea-Indonesia and Philippine waters, where in addition to high primary productivity levels, most of the energy is transferred to the upper layer since there are no bathy- and meso-pelagic layers. When comparing the biomass distribution in the different layers, there is an obvious contrast between forage biomass in the epi- and bathy-pelagic layers during the day (Fig. 5), most of the biomass being concentrated in the deepest layer (Fig. 6). The average spatial distribution of bathypelagic biomass is more diffuse with a contrast between a rich cold-tongue associated with the

equatorial upwelling and merging in the east with the highly productive coastal upwelling along the Peruvian coast and lower biomass on each side in the central gyres.

The contrasts in spatial distribution are also associated with time lags in the turn-over of the mid-trophic components. For example, low and high peaks in primary production are propagated with a delay of ~2 months in the epipelagic component in the equatorial east Pacific, but because of the cold temperature in the deep layer, the lag increases to 12-14 months for the bathypelagic group (Fig. 5). These differences can lead to opposite peaks in the fluctuation of epipelagic and bathypelagic groups (Fig 5) and complex spatial heterogeneity due to redistribution by oceanic circulation.

In addition to their own internal dynamics, the mid-trophic components are affected by the interannual and longer time scale variability of climate and the environment, through changes in temperature, currents and primary production. These changes are reproduced by the physical-biogeochemical model (Fig. 4) and the effects on mid-trophic components illustrated in Figure 6, where biomass time series of the 6 mid-trophic components are provided for the equatorial box 5°N-5°S; 120°W-100°W. With different time lags, all components are affected by ENSO-related interannual variability (e.g. El Niño events of 1972-73, 1982-33 and 1997-98, and La Niña events of 1988-89 and 1999-2000). The amplitude of ENSO-related fluctuations decreases through the mid-trophic groups in relation with the proportion of time spent in the upper layers, i.e. that groups with higher turnovers and low biomass over production ratio are more affected than groups with lower turnovers and high B/P ratios (Fig. 6). Considering all the mid-trophic groups together, the sum of their anomalies relatively to the mean biomass of each group is correlated to the Southern Oscillation Index (SOI) with a maximum coefficient of correlation ($r = 0.64$) for a time lag of 6 months. Interestingly, frequency of the ENSO signal is smoothed through the different mid-trophic groups, leading to decadal periods dominated by positive (1950-1977) or negative (1978-1999) anomalies, the last one being positive and starting in 2000. This cascade of ENSO influences through the mid-trophic levels needs further validation against observations even though there are only sparse observations.

On the spatial scale, the ENSO variability, characterized by large changes in surface circulation, temperature distribution and primary production (Fig. 3), strongly affects the forage biomass distribution in the tropical regions (Fig. 7). For example, at the end of the last strong El Niño event of 1997-1998, the simulation predicts an interesting asymmetric distribution of epipelagic biomass relative to the equator with an enhanced biomass west of the Dateline, and conversely a more strongly depleted southern subtropical gyre. This pattern is observed both for day and night distributions (Fig. 7) with in addition a substantial increase of biomass at night in the eastern Pacific Ocean. At night, the biomass in the upper layer increases by a factor 6 to 10 due to migration of meso- and bathy-pelagic components (Fig. 7).

### 4.2. Evaluation

Despite the wide spatio-temporal distribution and huge abundance of mid-trophic level organisms and their major influence on top predator distribution and population dynamics, they are still one of the less known components of pelagic ecosystems. The first source of observation that can be used for the parameterization of the model and the evaluation of its outputs are biomass estimates from different micronekton sampling cruises. Because time and cost constraints, as well as difficulty inherent to net sampling techniques (e.g. collect the most agile organisms such as squids), these sparse observations provide only part of the picture.

Nevertheless, they are essential data providing a first order estimate of the absolute biomass of micronekton in the water column. For example, the EASTROPAC cruises in 1967-1968 (Blackburn and Laurs, 1972) provided distributions of micronekton in the eastern equatorial Pacific Ocean (EPO) in the upper 200m showing an increase in biomass between day and night from ~1-8 to 10-20 ml/1000 $m^3$, and still some higher concentration near the coast of Peru. Assuming a conversion of 1g per ml and since the epipelagic layer here is 100m, this leads to value of 0.1-0.8 and 1-2 gWW $m^{-2}$ for day and night respectively, which is consistent with the model outputs (Fig. 7).

On the other side of the basin, Hidaka et al. (2003) sampled in the warm pool, north of Papua New Guinea (0°-10°N; 140°E-150°E) during a cruise in Jan.-Feb. 1998. They calculated that the micronekton biomass in the upper 200 m was in general <1 mg WW $m^{-3}$ (0.01-0.7 mg WW $m^{-3}$) during the day, with a few exception when large schools of epipelagic anchovy were encountered (max. value 23.3 mg WW $m^{-3}$), and increased to a range of 3-38.8 mg WW $m^{-3}$ at night. Here, after converting to g WW $m^{-2}$ for a 100 m epipelagic layer (i.e., multiplying by 100 m and dividing by 1000 mg), we obtain a range of 0.001-0.07 and 0.3-3.88 mg WW $m^{-2}$ for day and night respectively that are in the same order of predicted values as shown on figure 7 (7a and 7b).

With the development of acoustic techniques and surveys, the use of micronekton net sampling has become a useful method to calibrate and standardize the biomass integration from the acoustic signal. However, the simulated migrant pelagic biomass includes all type of organisms while acoustic data frequently target one group of species, e.g., mesopelagic fishes (McClatchie and Dunford, 2003). Thus, these surveys provide a useful but still rough evaluation and require careful calibration. Nonetheless, acoustic studies offer the considerable advantage of potentially providing long time series of data. As an illustration of the interest of acoustic monitoring for model evaluation, we compared the backscatter signal of ADCP (Acoustic Doppler Current Profiler) that was deployed on the TAO-TRITON array of oceanographic buoys at two locations on the Equator, at 165$^o$E and 170$^o$W, with primary production and biomass of mid-trophic components in the epipelagic layer at night, both predicted from the simulation above (Fig. 8). ADCP backscatter signal is linked to the biomass of macrozooplankton (roughly >1cm) and micronekton and thus is an abundance index of the mid-trophic organisms. The comparison shows that fluctuations of the ADCP time series are delayed by approximately two months relative to the predicted primary production. This is a coherent result given the expected delay between primary and secondary/tertiary production. Conversely, these fluctuations match very well those of the predicted mid-trophic biomass suggesting that the model captures the important spatio-temporal dynamics of these groups.

While we will continue, for the evaluation of the model outputs, to compile more of these direct and indirect measures of mid-trophic biomass. Furthermore, we will search for an approach to use long time series of acoustic profiles to be processed and directly assimilated in the model for parameter optimization. This will require identifying the functional groups in the echograms and to extract the corresponding part of the signal.

## 5. Discussion

Organisms occupying the mid-trophic level either temporarily or permanently during their life can be both prey of larger predators but also predators or smaller organisms, including eggs, larvae and small-size juveniles of marine pelagic species. Therefore, they can potentially control the

dynamics of all marine species through different mechanisms, which can produce complex results, when interacting in a dynamic system.

First, mid-trophic organisms are prey of large oceanic species that are essentially opportunistic omnivorous predators. Most of these large predators are in the upper layer during the night, while during the day species have evolved to exploit different though overlapping vertical layers. If we consider the schematic view of the pelagic system with three vertical layers: epi-, meso- and bathy-pelagic, as used to describe the mid-trophic components in the present study, it is relatively easy to roughly classify different vertical behavior types of top predators according to their ability to explore the deeper layers. Thus, both horizontal and vertical distributions of prey fields are certainly key factors to understand the spatio-temporal dynamics of the large oceanic predator species, and the modelling approach presented here offers an ideal framework for developing new generation of spatially-explicit population dynamic models of exploited oceanic predators of micronekton.

One example of coupling a fish population dynamic model to this suite of models representing ocean physics to lower and mid-trophic levels is the spatial ecosystem and populations dynamics model SEAPODYM (Lehodey et al., 2003; Lehodey et al., 2008). It uses the functional mid-trophic components above for constraining the spatial dynamics of predators (e.g., tuna) and the food competition between the predator species. The model also includes a description of multiple fisheries and then predicts spatio-temporal distributions of catch, catch rates, and length-frequencies. Thus, it becomes possible to use fishing data for model parameters optimisation and test if the mechanisms included into the deterministic model can be justified from available data (Senina et al., 2008). At the difference of standard statistical population dynamic models, such spatially-explicit models driven by environmental mechanisms provide the ability to perform hindcast and forecast simulations, forced by reanalyses or projections of environmental variables, an thereby to explore long-term scale variability due to interannual and decadal climate variability or impacts of global warming.

While adult large oceanic species are likely searching for concentrations of mid-trophic organisms to feed, they should try to avoid them for spawning to increase the chance of their own larvae to survive and to be then recruited into the adult population. Understanding the recruitment mechanisms in marine species has been and still is one of the most important research fields in fishery sciences. Briefly, the key mechanisms include the problem of starvation, especially since the larval phase appears as a critical period (Hjort, 1914). Cushing (1975) thus introduced the concept of match-mismatch between spawning and presence of food for larvae, to explain recruitment variability. The temperature that influences growth rates, and thus the duration of this critical life period, is also of primary importance. Considering the dynamic oceanic environment, advection becomes an issue since oceanic circulation can create retention or dispersion in favourable or unfavourable zones (Parrish et al. 1983). Surprisingly, there are very few studies that investigate the relationship between recruitment and the predation of larvae. One reason is likely the difficulty of sampling the predators of larvae (i.e. the mid-trophic biomass essentially) comparatively to the sampling of their prey (phyto- and zooplankton). A realistic modelling of the mid-trophic biomass would certainly help in investigating the role of predation in larvae survival, and could also assist in the preparation of research cruises.

A key issue for the coming years will be to compile all available information allowing to evaluate and to calibrate this type of mid-trophic models based on functional groups or other approaches, e.g., a continuous size spectrum ( Maury et al., 2007). But new tools are also needed, based on existing technology for large scale monitoring of these mid-trophic level organisms. Ultimately,

collected data should be used for parameters optimization and data assimilation. A recent workshop[1] initiated by the CLIOTOP programme discussed the observational needs for addressing this critical lack of information. The purpose of this meeting was to identify the requirements for addressing the first phase of development of a generic automated acoustic sampler of the open ocean mid-trophic organisms (the MAAS) in the perspective of a second phase devoted to its large scale deployment on drifter networks. Aimed to improve and validate mid-trophic models the acoustic observations provided by the MAAS were listed in the order of difficulty to achieve:

1. the vertical distribution of the biomass and the depth of the different biological layers including their daily vertical migrations;
2. the relative abundance indices for each depth layer;
3. the absolute abundance indices for the depth layers;
4. rough taxonomic group identifications in the depth layers (e.g.: myctophids, crustaceans, cephalopods, jellyfish, etc.);
5. the size distribution of biomass within the depth layers.

The use of acoustic data has often been criticized due to the difficulty of getting reliable estimates of absolute biomass and identification of taxonomic groups with this technology. However, a consistent estimation of relative distribution of biomass in the vertical layers seems a realistic objective that can be achieved. This would offer critical information for model parameterization, as relative changes in day and night biomass values in each vertical layer provide information to aid the parameterization of energy efficiency coefficients in different oceanic regions, in particular through data assimilation techniques. Stable isotope analyses are the other valuable source of information to assess energy transfer from primary production to upper trophic levels (Jennings et al. 2002) including the mid-trophic groups, and are particularly well suited for comparisons with model outputs based on carbon or nitrogen cycles.

It is worth noting that even without absolute estimates, relative spatio-temporal distributions of mid-trophic biomass have a large range of applications, from investigating horizontal and vertical behaviors and habitats of large predators of these mid-trophic level species to the coupling with spatial population dynamics of these same species, based on relative rather than quantitative mechanisms. For example, the match/mismatch between spawning and presence of food larvae can be combined in a model with the larvae predation effect by the use of a ratio between food (zooplankton) and predators (mid-trophic organisms) of larvae (e.g., see an application in Lehodey et al., 2008).

With an increasing amount of data for model parameterization it will become possible to envisage the full coupling of the mid-trophic functional groups to the biogeochemical model, i.e., to parameterize the transfer from zooplankton and detritus groups in one way and the flux of mid-trophic groups to the detritus component in the other way. A proper parameterization will be strongly dependent on the availability of the acoustic data. The main advantage of such coupling could be for the biogeochemical modelling, where a more realistic spatio-temporal variability of zooplankton mortality rate could be expected, since it would be linked to the biomass of predicted mid-trophic components.

Finally, unexpected applications can originate from the modelling of mid-trophic components. One example is the study of biological turbulence in the sea. This stimulating idea has been

[1] "Designing an Ocean Mid-trophic Automatic Acoustic Sampler (MAAS)" workshop, Sète, France, Jan 15-18, 2007. The report is available on the CLIOTOP web site (www.globec.org/regional/)

regenerated recently by the measured contribution of krill turbulence in an inlet of British Columbia (Kunze et al., 2006), which showed local increases by three to four orders of magnitude. These measurements bring new interest on more theoretical findings by Huntley and Zhou (2004) who calculated the rate of turbulent kinetic energy production by various species encompassing a large range of size (from krill to tuna and whales). A significant large-scale biological feedback on the ocean turbulence due to the vertical migration of the huge biomass of meso- and bathy-pelagic organisms would be a fundamental discovery and is thus worth exploring. Numerical simulations combining an estimate of the biomass of these organisms and their potential production of turbulent kinetic energy (TKE) – e.g., following Huntley and Zhou (2004) approach – could provide a first insight on the potential large-scale effect of animal-induced turbulence in the ocean. This additional TKE production term could then be simply added in the TKE budget that governs vertical mixing (e.g., Gaspar et al., 1990). Then, in situations where biological production significantly augments the TKE level, the simulated vertical mixing will be enhanced. This will generally induce an increased injection of cold, nutrient-rich, water from the pycnocline into the euphotic layer which could, in turn, yield an enhanced primary production and, ultimately, an increased mass of turbulence-producing organisms. The importance of such retroactions can certainly be explored using the type of simple mid-trophic model presented here.

In conclusion, the present modeling approach proposed to bridge the gap from ocean models to population dynamics of large predators is likely one of the most simple that can be proposed, with strengths and weaknesses as for any other approach. It certainly requires an important effort of evaluation and parameterization, but at least the minimum number of required parameters makes this effort possible even in the context of limited observations.

## Acknowledgments

The authors would like to thank IGBP programs GLOBEC and IMBER as well as the Network of Excellence EUR-OCEANS of the European Union's 6th Framework Program for funding the symposium on "Parameterization of Trophic Interactions in Ecosystem Modelling", Cadiz, March 2007, and the meeting conveners for the invitation to participate. This work was supported by the European-funded Pacific Regional Oceanic and Coastal Fisheries Development Programme (PROCFish) of the Oceanic Fisheries Programme of the Secretariat of the Pacific Community, New Caledonia, and the Marine Ecosystems Modeling and Monitoring by Satellite section in CLS, France. It has also beneficiated of a research grant (# 651438) from the JIMAR-Pelagic Fisheries Research Program of the University of Hawaii at Manoa, USA. The authors thank Michael Mc Phaden and Patricia Plimpton from the NOAA/PMEL and Marie-Hélène Radenac from IRD for kindly providing ADCP data and assisting in their analysis. We also thank the anonymous reviewers who contributed to a significant improvement of the original manuscript.

## References

Abookire, A. A., Piatt, J. F., & Speckman, S. G. (2002). A nearsurface, daytime occurrence of two mesopelagic fish species (*Stenobrachius leucopsarus* and *Leuroglossus schmidti*) in a glacial fjord. *Fishery Bulletin*, **100**: 376-380.

Alheit, J., & Hagen, E. (1997). Long-term climate forcing of European herring and sardine populations. *Fisheries Oceanography*, **6**(2): 130-139.

Allain, G. (2005). Modélisation biophysique pour la prévision du recrutement. Couplage stochastique d'un modèle individu-centré de croissance larvaire avec un modèle hydrodynamique 3D pour développer un indice de recrutement de l'anchois dans le golfe de Gascogne. Thèse de doctorat. Ecole Nationale Supérieure Agronomique de Rennes. France. 183 pp.

Allen, K. R. (1971). Relation between production and biomass. *Journal of the Fisheries Research Board of Canada*: ***28***, 1573–1581.

Belgrano, A., Allen, A.P., Enquist, B. J., & Gillooly, J. F. (2002). Allometric scaling of maximum population density: a common rule for marine phytoplankton and terrestrial plants. *Ecology letters*, **5**: 611-613.

Blackburn, M. (1968). Micronekton of the eastern tropical Pacific Ocean: family composition, distribution, abundance, and relations to tuna. *Fishery Bulletin U.S*., **67**: 71-115.

Blackburn, M., & Laurs, M. R. (1972). Distribution of forage of skipjack tuna (*Euthynnus pelamis*) in the eastern tropical Pacific. NOAA No. SSRF-649.

Boudreau, P. R., & Dickie, L. M. (1992). Biomass spectra of aquatic ecosystems in relation to fisheries yield. *Canadian Journal of Fisheries and Aquatic Sciences,* **46**: 614-623.

Brown, J. H., Gilooly, J. F., Allen, A. P., Savage, V. M., & West, G. (2004). Toward a metabolic theory of ecology. *Ecology*, **85**: 1771-1789.

Butterworth, D. S., & Plaganyi, E. E. (2004). A brief introduction to some approaches to multispecies/ecosystem modeling in the context of their possible application in the management of South African fisheries. *Afr. J. mar. Sci.,* **26**: 53–61.

Carscadden, J., Nakashima, B. S., & Frank, K. T. (1997). Effects of fish length and temperature on the timing of peak spawning in capelin (*Mallotus villosus*). *Canadian Journal of Fisheries and Aquatic Sciences,* **54**: 781-787.

Chai, F., Dugdale, R. C., Peng, T-H., Wilkerson, F. P., & Barber, R. T. (2002). One Dimensional Ecosystem Model of the Equatorial Pacific Upwelling System, Part I: Model Development and Silicon and Nitrogen Cycle. *Deep Sea Research II,* **49**: 2713-2745.

Chen, D., Rothstein, L. M., & Busalacchi, A. J. (1994). A hybrid vertical mixing scheme and its application to tropical ocean models. *Journal of Physical Oceanography*, **24**: 2156-2179.

Christensen, V., & Pauly, D. (1992). Ecopath II - a software for balancing steady-state ecosystem models and calculating network characteristics. *Ecol. Model*. **61**, 169–185.

Christian, J., Verschell, M., Murtugudde, R., Busalacchi, A., & McClain, C. (2002). Biogeochemical modeling of the tropical Pacific Ocean I: Seasonal and interannual variability. *Deep Sea Research II*, **49**: 509-543.

Christian, J. R., & Murtugudde, R. (2003). Tropical Atlantic variability in a coupled physical-biogeochemical ocean model. *Deep Sea Research II*, **50**(22-26): 2947-2969.

Coale, K. H., Johnson, K. S., Fitzwater, S. E., & 16 co-authors (1996). A massive phytoplankton bloom induced by an ecosystem-scale iron fertilization experiment in the Equatorial Pacific Ocean. *Nature* **383**: 495-501.

Cushing, D. H. (1975). *Marine ecology and fisheries*. Cambridge Univ. Press, Cambridge, England, 278 p.

Dalzell, P. J. (1993). Small pelagic fishes. *In* Wright A. & Hill, L., *Nearshore marine resources of the South Pacific* (pp. 97–133). Canada: IPS, Suva, FFA, Honiara, ICOD.

Dickie, L. M. (1976). Predation, yield and ecological efficiency in aquatic food chains. *Journal of the fisheries Research Board of Canada* **33**: 313-316.

Dugdale, R. C., Barber, F., Chai, F., Peng, T. H., & Wilkerson, F.P. (2002). One dimensional ecosystem model of the equatorial Pacific upwelling system, Part II: Sensitivity analysis and comparison with JGOFS EqPac Data. *Deep Sea Res. II* **49** (13-14):2746-2762.

Elton, C. (1927). *Animal ecology*. Macmillan, New York, NY. 207 pp.

Enquist, B. J., Brown, J. H., & West, G. B. (1998). Allometric scaling of plant energetics and population density. *Nature*, **395**: 163–165.

Fenchel, T. (1974). Intrinsic rate of natural increase: the relationship with body size. *Oecologia*, **14**: 317-326.

Forsythe, J. W., Walsh, L. S., Turk, P. E., & Lee, P. G. (2001). Impact of temperature on juvenile growth and age at first egg-laying of the Pacific reef squid *Sepioteuthis lessoniana* reared in captivity. *Marine Biology,* **138**: 103-112.

Froese, R., & Binohlan, C. (2000). Empirical relationships to estimate asymptotic length, length at first maturity and length at maximum yield per recruit in fishes, with a simple method to evaluate length frequency data. *Journal of Fish Biology* 56, 758–773.

Gaspar, P., Grégoris, Y., & Lefevre, J. M. (1990). A simple eddy-kinetic energy model for simulations of the oceanic vertical mixing: tests at Station Papa and Long-Term Upper Ocean Study Site. *J. Geophys. Res.,* **95**: 16179-16193.

Gillooly, J. F., Charnov, E. L., West, G. B., Savage, V.M., & Brown, J. H. (2002). Effects of size and temperature on developmental time. *Nature*, **417**: 70–73.

Grandperrin, R. (1975). Structures trophiques aboutissant aux thons de longues lignes dans le Pacifique sud-ouest tropical. Thèse de Doctorat, Université de Marseille.

Hansen, H. O., & Aschan, M. (2000) Growth, size and age-at-maturity of shrimp, *Pandalus borealis*, at Svalbard, related to environmental parameters. *Journal of Northwestern Atlantic Fisheries Science*, **27**: 83-91.

Hidaka, K., Kawaguchi, K., Tanabe, T., Takahashi M., & T., Kubodera (2003). Biomass and taxonomic composition of micronekton in the western tropical-subtropical Pacific. *Fisheries Oceanography*, **12**(2): 112-125.

Hjort, J. (1914). Fluctuations in the great fisheries of northern Europe. *Rapp. P.-V. Reun. Cons. Int. Explor. Mer* **20**:1–227.

Hunter, J.R., & Wada, T. (Eds), (1993). PICES Scientific Report No. 1. Part 1. Coastal pelagic fishes. Publish. North Pacific Marine Science Organisation (PICES), 131 pp.

Huntley, M. E., & Zhou, M. (2004). Influence of animals on turbulence in the sea. *Marine Ecology Progress Series*, **273**: 65–79.

Ichii, T., Mahapatra, K., Sakai, M., Inagake, D., & Yoshihiro, O. (2004). Differing body size between the autumn and the winter–spring cohorts of neon flying squid (*Ommastrephes bartramii*) related to the oceanographic regime in the North Pacific: a hypothesis. *Fisheries Oceanography,* **13** (5): 295-309.

Ikeda, T. (1992). Growth and life history of the mesopelagic mysid *Meterythrops microphthalma* in the southern Japan Sea. *Journal of Plankton Research,* **14**(12): 1767-1779.

Iverson, R.L. (1990). Control of marine fish production. *Limnology Oceanography* **35**:1593-1604.

Jackson, G. D., & Choat, J.H. (1992). Growth in tropical cephalopods: an analysis based on statolith microstructure. *Canadian Journal of Fishery and Aquatic Sciences,* **49:** 218–228.

Jackson, G. D., & Moltschaniwskyj, N.A. (2002). Spatial and temporal variation in growth rates and maturity in the Indo-Pacific squid *Sepioteuthis lessoniana* (*Cephalopoda: Loliginidae*). *Marine Biology*, **140**: 747-754.

Jennings, S., Warr, K. J., & Mackinson, S. (2002). Use of size-based production and stable isotope analyses to predict trophic transfer efficiencies and predator-prey body mass ratios in food webs. *Marine Ecology Progress Series*, **240**: 11–20.

Kerr, S. R. (1974). Theory of size distribution in ecological communities. *J. Fish. Res. Bd. Can*., **31**:1859-1862.

King, J. E., & Iversen, R.T.B. (1962). Midwater trawling for forage organisms in the central Pacific, 1951-1956. *Fishery Bulletin. U.S.,* **210**: 271-321.

Kleiber, M. (1932). Body size and metabolism. *Hilgardia,* **6**: 315–353.

Kobayashi, H. A. (1974). Growth Cycle and Related Vertical Distribution of the Thecosomatous Pteropod *Spiratella ("Limacina") helicina* in the Central Arctic Ocean. *Marine Biology* **26:** 295-301.

Kooijman, S. A. L. M. (1986). Energy budgets can explain body size relations. *J. Theor. Biol.,* **121**: 269–282.

Kunze E., Dower J. F., Beveridge I., Dewey R., & Bartlett K. P. (2006). Observations of biologically generated turbulence in a coastal inlet. *Science*, **313**(5794): 1768-1770.

Legand, M., Bourret, P., Fourmanoir, R., Grandperrin, R., Gueredrat, J. A., Michel, A., Rancurel, P., Repelin, R., & Roger, C. (1972). Relations trophiques et distributions verticales en milieu pélagique dans l'Océan Pacifique intertropical. *Cahier ORSTOM, Série Océanographique*, **10**(4): 303-393.

Lehodey, P., Andre, J-M., Bertignac, M., Hampton, J., Stoens, A., Menkes, C., Memery, L., & Grima, N. (1998). Predicting skipjack tuna forage distributions in the equatorial Pacific using a coupled dynamical bio-geochemical model. *Fisheries Oceanography,* **7**(3/4):317-325.

Lehodey, P., Chai, F., & Hampton, J. (2003). Modeling climate-related variability of tuna populations from a coupled ocean-biogeochemical-populations dynamics model. *Fisheries Oceanography,* **12**(4): 483-494.

Lehodey, P. (2001). The pelagic ecosystem of the tropical Pacific Ocean: Dynamic spatial modeling and biological consequences of ENSO. *Progress in Oceanography,* **49:** 439-468.

Lehodey, P. (2004a). Climate and fisheries: an insight from the Pacific Ocean. *In Ecological effects of climate variations in the North Atlantic*, Stenseth N.C., Ottersen G., Hurrel J. and Belgrano A. (Eds.) Oxford University press: 137-146.

Lehodey, P. (2004b) A Spatial Ecosystem And Populations Dynamics Model (SEAPODYM) for tuna and associated oceanic top-predator species: Part I – Lower and intermediate trophic components. 17th meeting of the Standing Committee on Tuna and Billfish, Majuro, Republic of Marshall Islands, 9-18 Aug. 2004, Oceanic Fisheries Programme, Secretariat of the Pacific Community, Noumea, New Caledonia, *SCTB Working Paper*: **ECO-1**: 26 pp.

Lehodey, P., Senina, I., & Murtugudde, R. (2008). A Spatial Ecosystem And Populations Dynamics Model (SEAPODYM) – Modeling of tuna and tuna-like populations. *Progress in Oceanography*, **78**: 304-318.

Lindeman, R. L. (1942). The trophic-dynamic aspect of ecology. Ecology 23: 399-418.

McClatchie, S., & Dunford, A. (2003). First estimate of the biomass of vertically migrating mesopelagic fish off New Zealand. *Deep Sea Res. I,* **50**: 1263-1281.

Maier-Reimer, E. (1993). Geochemical cycles in an ocean general circulation model. Preindustrial Tracer Distributions. *Global Biogeochemical Cycles*, **7**: 645-677.

Martin, J. H., Coale, K. H., Johnson, K. S., Fitzwater, S. E., & 40 authors (1994). Testing the iron hypothesis in ecosystem of the equatorial Pacific Ocean. *Nature*, **371**, 123-129.

Martin, J. H. (1990). Glacial-interglacial CO2 change: The iron hypothesis. *Paleoceanography*, 5(1): 1-13.

Maury, O., Faugeras, B., Shina, Y-J., Poggialeb, J-C., Ben Aria, T., & Marsac, F. (2007). Modeling environmental effects on the size-structured energy flow through marine ecosystems. Part 1: The model. *Progress in Oceanography*, *74,* 479-499.

Murtugudde, R., Beauchamp, J., McClain, C., Lewis, M., & Busalacchi, A. J. (2002). Effects of penetrative radiation on the upper tropical ocean circulation. *Journal of Climate,* **15:** 470-486.

Murtugudde, R., Seager, R., & Busalacchi, A. (1996). Simulation of the tropical oceans with an ocean GCM coupled to an atmospheric mixed layer model. *Journal of Climate,* **9**: 1795-1815.

Murtugudde, R. G., Wang, L., Hackert, E., Beauchamp, J., Christian, J. R., & Busalacchi, A. J. (2004). Remote sensing of the Indo-Pacific region: Ocean color, sea level, winds, and SSTs. International Journal of Remote Sensing **25**(7-8): 1423-1435.

Palomares, M.L., Muck, P., Mendo, J., Chuman, E., Gomez, O., & Pauly, D. (1987). Growth of the Peruvian anchoveta (*Engraulis ringens*), 1953 to 1982. *In*: Pauly, D., Tsukayama, I.

(eds) The Peruvian anchoveta and its upwelling ecosystems: three decades of change, vol 15, pp 117-141

Parrish, R. H., Bakun, A., Husby, D. M., & Nelson, C.S. (1983). Comparative climatology of selected environmental processes in relation to eastern boundary current pelagic fish reproduction. (Proc. The Expert Consultation to Examine Changes in Abundance and Species Composition of Neritic Fish Resources, San JoseÂ, Costa Rica). *FAO Fish. Rep*. **293**(3): 731-777.

Platt, T., & Denman, K. L. (1978). The structure of the pelagic marine ecosystems. *Rapp. P.-V. Réunion Du Conseil International pour l'Exploration de la Mer* **173**: 60-65.

Platt, T. (1985). Structure of the marine ecosystem: its allometric basis. *Canadian Bulletin of Fisheries and Aquatic Sciences* **213**: 55-64.

Plimpton, P. E., Freitag, H. P., & McPhaden, M. J. (2004). Processing of Subsurface ADCP Data in the Equatorial Pacific. /NOAA Tech. Mem./OAR PMEL-125, 41 pp.

Prager, M. H., & MacCall, A. D. (1988). Revised estimates of historical spawning biomass of the Pacific mackerel, *Scomber japonicus*. *CalCOFI Reports* **29**: 81-90.

Reid, R. N., Cargnelli, L. M., Griesbach, S. J., Packer, D. B., Johnson, D. L., Zetlin, C. A., Morse, W. W., & Berrien, P. L. (1999). Essential Fish Habitat Source Document: Atlantic Herring, *Clupea harengus*, Life History and Habitat Characteristics. *US NOAA Technical Memorandu*m NMFS **NE-126**: 56 pp.

Repelin, R. (1978). Les amphipodes pélagiques du Pacifique occidental et central: Biologie, écologie et relations trophiques avec la faune ichthyologique. *Travaux et Documents de l'ORSTOM*, **86**: 381 pp.

Ricker, W. E. (1975). Computation and interpretation of biological statistics of fish populations. *Bulletin of Fisheries Research Board Canada.* **191**: 382 pp.

Roger, C. (1971). *Les euphausiacés du Pacifique équatorial et sud tropical*. Thèse de Doctorat, Université de Provence - ORSTOM.

Samsun, O., Samsun, N., & Karamollaoglu, A. C. (2004). Age, growth and mortality rates of the European anchovy (*Engraulis encrasicolus,* L. 1758) off the Turkish Black Sea coast. *Turkish Journal of Veterinary and Animal Science*, **28**: 901-910.

Savage, V. M., Gilllooly, J. F., Brown, J. H., West, G. B., & Charnov, E. L. (2004). Effect of body size and temperature on population growth. *The American naturalist*, **163**(3): 429-441.

Schwartzlose, R. A., Alheit, J., Bakun, A., Baumgartner, T. R., & 17 authors (1999). Worldwide large-scale fluctuations of sardine and anchovy populations. *South African Journal of Marine Sciences,* **21**: 89–347.

Senina, I., Sibert J., & Lehodey, P. (2008). Parameter estimation for basin-scale ecosystem-linked population models of large pelagic predators: Application to skipjack tuna. *Progress in Oceanography,* **78**: 319-335.

Sheldon, R. W., Prakash, A., & Sutcliffe Jr, W. H. (1972). The size distribution of particles in the Ocean. *Limnology Oceanography*, **17**: 327–340.

Sibert, J. R., Hampton, J., Fournier, D. A., & Brills, P. J. (1999). An advection-diffusion-reaction model for the estimation of fish movement parameters from tagging data, with application to skipjack tuna (*Katsuwonus pelamis*). *Canadian Journal of Fisheries and Aquatic Sciences,* **56**: 925-938.

Siegel, V. (2000). Krill *(Euphausiacea)* life history and aspects of population dynamics. *Canadian Journal of Fishery and Aquatic Sciences,* **57**(Suppl. 3): 130-150.

Stéquert, B., Ménard, F., & Marchal, E. (2003). Reproductive biology of *Vinciguerria nimbaria* in the equatorial waters of the eastern Atlantic Ocean. *Journal of Fish Biology*, **62**: 1116-1136.

Takahashi, M., & Watanabe, Y. (2004). Growth rate-dependent recruitment of Japanese anchovy *Engraulis japonicus* in the Kuroshio-Oyashio transitional waters. *Marine Ecology Progress Series*, **266**: 227-238.

Van der Meer, J. (2006). Metabolic theories in ecology. *Trends in ecology and evolution*, **21**(3): 136-140.

Vinogradov, M. E. (1981). Ecosystems of equatorial upwellings. In *Analysis of Marine Ecosystems*. Edited by A.R.Longhurst. Academic Press, pp. 69-93.

Wang, X., Christian, J. R., Murtugudde, R., & Busalacchi, A. J. (2005). Ecosystem dynamics and export production in the central and eastern equatorial Pacific: A modeling study of impact of ENSO. *Geophysical Research Letter*, **32**, L2608.

Wang, X., Christian, J. R., Murtugudde, R., & Busalacchi, A. J. (2006a). Spatial and temporal variability of the surface water pCO(2) and air-sea CO2 flux in the equatorial Pacific during 1980-2003: a basin-scale carbon cycle model. *Geophysical Research Letter*, **111**, C07S04.

Wang, X., Christian, J. R., Murtugudde, R., & Busalacchi, A. J. (2006b). Spatial and temporal variability in new production in the equatorial Pacific during 1980-2003: physical and biogeochemical controls. *Deep Sea Research II*, **53**: 677-697.

West, G. B., Brown, J. H., & Enquist, B. J. (1997). A general model for the origin of allometric scaling laws in biology. *Science* **276**: 122-126.

West, G. B., Brown, J. H., & Enquist, B. J. (2001). A general model for ontogenic growth. *Nature* **413**: 628-631.

Wiggert, J. D., Murtugudde, R., & Christian, J. R. (2006). Annual ecosystem variability in the tropical Indian Ocean: results of a coupled bio-physical ocean general circulation model. *Deep Sea Research* **53**: 644-676.

Wood, J. B., & O'Dor, R. K. (2000). Do larger cephalopods live longer? Effects of temperature and phylogeny on interspecific comparisons of age and size at maturity. *Marine Biology*, **136**: 91-99.

## Appendix A. Taxonomic classification based on the definition of functional components

Based on several seminal works carried out in the Pacific Ocean by Blackburn (1968), Granperrin (1975), King and Iversen (1962), Legand et al. (1972), Roger (1971), and Vinogradov (1981), the pelagic micronekton has been divided into epipelagic, mesopelagic and bathypelagic groups, the last two groups being subdivided into migrant and non-migrant species. These groups include organisms of the main taxa (**Table A-1**): fish, crustacean, cephalopods and the gelatinous filter feeders.

Table A-1. Mid-trophic species and taxa of the tropical Pacific Ocean classified by vertical migrant or non-migrant components, based on King and Iversen (1962), Roger (1971), Legand et al. (1972), Blackburn and Laurs (1972), Granperrin (1975), and Repelin (1978)

| | |
|---|---|
| ***Epipelagic layer*** | |
| Crustaceans: | o small size (< 20 mm) euphausids (e.g., *Stylocheiron carinatum*, *Euphausia tenera*, *S. affine*)<br>o larvae of crabs, shrimps, and stomatopods<br>o pelagic adult decapods (in particular, the pelagic phase of the red crab (*Pleurocondes planipes*) is very abundant in the Eastern Pacific and represents an important source of food for skipjack)<br>o Almost all amphipods of the family Phronimidae. |
| Fish: | o Engraulidae (anchovies) – The oceanic anchovy (*Enchrasicholinus punctifer*) seems to be a key species in the epipelagic food chain in the warmpool as it is growing very quickly (mature after 3-5 months) and can become very abundant after episodic blooms of phytoplankton.<br>o Clupeidae (herrings, sardines)<br>o Exocœtidae (flyingfish)<br>o small Carangidae (scads)<br>o all juvenile stages of large-size species (Bramidae, Coryphaenidae, Thunnidae, etc…). |
| Cephalopods: | o larval and juvenile stages of cephalopods<br>o small-size squids of the family Onychoteuthidae (*Onychoteuthis banksi, Onychia spp*.). |
| ***Mesopelagic Layer (migrant)*** | |
| Crustaceans: | o *Phronima sedentaria* - one of the species in the Phronimidae that does not stay in the epipelagic layer at day |
| Cephalopods: | o Enoploteuthidae |
| ***Mesopelagic Layer (permanent)*** | |
| Crustaceans: | o relatively few permanent species, like some euphausids (*Nematoscelis tenella, Stylocheiron maximum, S abbreviatum, S longicorn*) |
| ***Bathypelagic layer (migrant)*** | |
| Crustaceans: | o euphausids (*Nematoscelis microps, N. gracilis, Thynasopoda pectinata, T. rnonacantha T. orientalis and N. flexipes*)<br>o deep shrimps of the Peneidae |
| Fish: | o Melamphaidae (*Scopelogadus mizolepis, Scopelogadus sp*.)<br>o Myctophidae (*Lampanyctus niger*) |

| | |
|---|---|
| | o Gonostomatidae (*Gonostoma atlanticum, G. elongatum*)<br>o Chauliodidae (*Chauliodus sloani*)<br>o Percichthyidae (*Howella sp*.)<br>o Stomiatidae |
| ***Bathypelagic layer (highly migrant)*** | |
| Crustaceans: | o many euphausids (*Euphausia diomedae, Thysanopoda tricuspidata, T. aequalis, E. paragibba*)<br>o deep shrimps of the family Sergestidae |
| Fish: | o Myctophidae (*Ceratoscopelus warmingi, Diaphus elucens, D. bracycephalus, D. lucidus, D. mollis, Notolychnus valdiviae, Lobianchia gemellari*)<br>o Astronesthidae<br>o Melanostomiatidae<br>o Nemichthyidae<br>o Idiacanthidae (*Idiacanthus sp*.)<br>o Melamphaeidae (*Melamphaes sp*.)<br>o Gonostomatidae (*Vinciguerria nimbaria*) |
| ***Bathypelagic layer (permanent)*** | |
| Crustaceans: | o euphausids (*Nematoscelis boopis, Thysanopoda cristata, Bentheuphausia amplyops*)<br>o deep shrimps (Mysidaceae, Caridae) |
| Fish: | o Gonostomatidae (genus *Cyclothone*: *C. alba* and *C. microdon*, *Margrethia obtusirostra*)<br>o Myctophidae (*Taaningichthys sp*., *Diaphus anderseni*)<br>o Sternoptychidae (*Sternoptyx diaphana*)<br>o Trichiuridae (*Benthodesmus tenuis*)<br>o Scopelarchidae (*Scopelarchus guntheri*)<br>o Maurolicidae (*Valenciennelus tripunctulatus*) |
| Cephalopods: | o Cranchidae<br>o Chiroteuthidae<br>o Mastigoteuthidae<br>o Histioteuthidae<br>o Enoploteuthidae |

## Appendix B. Parameterization of energy efficiency coefficients

### 5.1. Total energy efficiency coefficient

Similar slopes in log-log biomass-body size (weight) relationships observed in different ecosystems (Dickie 1976, Boudreau and Dickie 1992) suggest that a simple parameterization can be used to define the energy transfer from primary production to upper trophic components, at least when they are not impacted by a too high external (fishing) forcing and include a sufficient diversity of organisms, allowing to compensate for species variability inside the ecological "size window" group. Considering the property of these biomass size spectra, it is not surprising that Iverson (1990), while compiling data in environments ranging from oceanic to coastal waters, calculated that for an average 2.5 trophic transfers from phytoplankton to carnivorous fish and squids (typically micronekton species) the annual production $F'_{yr}$ of these mid-trophic groups can be described according to a simple equation (*eq. 1*) based on annual primary production $P'_{yr}$, either from C transfer efficiency of total primary production or N transfer efficiency of new primary production.

$$F'_{yr} = P_{yr}' \cdot E^{2.5} \cdot c \qquad \text{(A1)}$$

When new primary production is used, $E$ appears to be a constant value (0.28), while it varies between 0.1 in oceanic environment and 0.2 in coastal environment for total primary production. These relationships have been used for the parameterization of energy transfer in our mid-trophic model. When using total primary production, we choose a value of 0.1 for the present basin-scale simulation. Coefficient $c$ is used to convert between units of N or C respectively to grams of fish wet weight.

For $P$ in mmol C, $c = 12 \times 10^{-3}$(g C) x 2.4 x 3.3 = 0.0948, with 2.4 the ratio between fish dry weight (g) and carbon (g) and 3.3 the ratio between fish wet weight(g) and fish dry weight (g) (from Vinogradov, in Iverson 1990).

For $P$ in mmol N, $c = 14 \times 10^{-3}$(g N) x 2.4 x 3.3 x 3.6 = 0.3992, with 3.6 the ratio between carbon and nitrogen in fish (from Vinogradov, cited in Iverson 1990).

### 5.2. Energy matrix coefficients

Coefficients of the energy matrix were estimated in several phases. First, a simple model with a single mid-trophic (forage) population integrating the biomass over all the vertical structure was used (Lehodey et al. 1998; Lehodey 2001; Lehodey et al. 2003) with predicted fields from two different coupled physical biogeochemical models: the carbon-based biogeochemical model used in the present study, and a nitrogen-based model (Chai et al., 2002; Dugdale et al., 2002). Interestingly, the comparison of average forage biomass predicted from these two different model configurations gave remarkably similar results, both in absolute values and in fluctuations in different equatorial geographical boxes (Lehodey 2004b).

Then, a 2-layer 3-component model was tested. In the absence of information on the level of energy transfer from primary production to each of the three components, a first simulation was run based on the 1-layer 1-component parameterization with equal part transferred to each component (i.e. 1/3, 1/3, 1/3). Results were compared to a few observations found in the

literature (Lehodey 2004b), e.g., the night and day distribution of micronekton in the eastern equatorial Pacific in the upper 200m as observed during EASTROPAC cruises in 1967-1968 (Blackburn and Laurs, 1972), leading to a new parameterization of 1/6 (epi), 3/6 (migrant) and 2/6 (deep).

Finally, simulations were run with the 3-layer 6-component model. Again the coefficient values were split between the new components and refined according to the same observations. In the special cases of shallow topography, the sum of transfer coefficients from forage components in the missing layer(s) is redistributed equally between the remaining components. The number of layers is identified from mask values in the input data files. Final matrix is provided in Table B-1.

Table B-1. Matrix of Energy transfer coefficients used for the 3-layer 6-components mid-trophic levels model, according to the depth and the number of corresponding layers

| | Mid-trophic functional groups | | | | | |
|---|---|---|---|---|---|---|
| Nb of Layers | epi | meso | m-meso | bathy | m-bathy | hm-bathy |
| 0 | 0 | 0 | 0 | 0 | 0 | 0 |
| 1 | 1 | 0 | 0 | 0 | 0 | 0 |
| 2 | 0.34 | 0.27 | 0.39 | 0 | 0 | 0 |
| 3 | 0.17 | 0.10 | 0.22 | 0.18 | 0.13 | 0.20 |

## Appendix C. Dynamics of mid-trophic functional components

The model is coupled "off-line" with biogeochemical model, that is, there is no feedback from the mid-trophic groups to the biogeochemical components (zooplankton or detritus). The recruits to each mid-trophic components $n$, i.e., production $F'_n$, are modeled by advection-diffusion equations, and their dynamics is driven by temperature and currents predicted by OGCM. These forcing variables as well as the calculated production are used then to drive "off-line" the numerical model of mid-trophic functional groups $F_n$.

### 5.3. Production model

The production $F_n'$ that contributes to the mid-trophic component $n$ is the cohort of organisms that are developing from primary production for the time $t_r$, and during this time are transported by water masses. The spatial dynamics can be described by simple advection-diffusion equation however the ageing of a cohort should also be considered assuming that age is linked to the ambient temperature (see section 2.3).

Let's denote $S_n$ the density of $n^{th}$ mid-trophic production component ($n$ = 1…6). At the time 'zero' the conversion according to Iverson formula (1) and energetic coefficient of Table B-1 is applied to primary production input. Then the development of micronekton production is governed by advection-diffusion equations during time $t_r$. Since the time $t_r$ depends on the ambient temperature, the age of a cohort varies in space. Thus, at each grid cell $ij$ of the model domain, $t_{r\,ij} = f\left(\hat{T}_{ij}\right)$, where function $f$ is derived from eq. (4) and symbol 'hat' denotes averaging over depth layers (see below). According to eq. (4), $t_r$ is smaller if the population inhabits the areas with high temperatures and larger for lower temperatures, with maximal value $t_{r\,max}$ = ¼ $t_{m\,max}$ fixed for the temperature of 0°C.

Space-dependence of the turn-over time together with the evidence that during this time mid-trophic production drifts in space with ocean currents and diffuses both with water masses and due to their own motions lead to the following discrete-continuous model:

$$\frac{\partial S_n^m}{\partial t} = D\left(\frac{\partial^2 S_n^m}{\partial x^2} + \frac{\partial^2 S_n^m}{\partial y^2}\right) - \frac{\partial}{\partial x}(\hat{u} S_n^m) - \frac{\partial}{\partial y}(\hat{v} S_n^m), \quad n = 1...6,\ m = 1...t_{r\max}$$

$$S_n^m = S_n^{m-1}, \text{for} \, 1 \le m \le \left\lfloor t_{r\,ij} \right\rfloor \qquad \text{(C1)}$$

where $D$ *is* the diffusion coefficient, $\hat{u}$ and $\hat{v}$ are the zonal and meridional components of the current. The set of equations (C1) is solved with initial condition

$$S_{nij}^0 = cE_n P_{ij}$$

and Neumann boundary conditions imposing impermeability of the domain:

$$\hat{u}_{ij} = \hat{v}_{ij} = \frac{\partial S_{ij}}{\partial x} = \frac{\partial S_{ij}}{\partial y} = 0, \quad \forall (i, j) \in \partial\Omega$$

Thus, in order to resolve both transport and ageing problems at the same time we introduce *m* variables $S_n^m$ ($m = t_{r\max} / \Delta t$ with *Δt*, the computational time step) for each mid-trophic group *n* which are simulated with help of discretized form of advection-diffusion equation, and at each time step yield to simple 'ageing' relationships according to instantaneous integer values of $t_{r\,ij}$ at each cell *ij*. The finite-difference approximation of ADEs is solved with alternate-direction-implicit method with monthly time step and one-degree grid spacing.

The averaging of the ocean currents as well as the ambient temperature is done according to the time the mid-trophic functional group is occupying its day or night layer, e.g.,

$$\hat{u} = \tau_d \cdot u_{dl} + (1 - \tau_d) \cdot u_{nl},$$

where $u_{dl}$ and $u_{nl}$ are the currents in day and night layer correspondingly, $\tau_d = DL / 24$ and the day length DL (nb of hours of daylight) is a function of the latitude φ (in radians) and the Julian day of the year J computed as (eq. C2 and C3, modified from Maier-Reimer 1993, pers com. L. Bopp):

$$DL = 24 - 2\,\mathrm{acos}(\mathrm{arg}) \cdot 180/\pi/15 \qquad [DL \geq 0] \qquad \text{(C2)}$$

with

$$\mathrm{arg} = \tan(\mathrm{asin}(\delta)) \cdot \tan(\varphi) \qquad [-1 \leq \mathrm{arg} \leq 1] \qquad \text{(C3a)}$$

and

$$\delta = \sin[2\pi\,(J-80)/365.25] \cdot \sin(\pi \cdot 23.5/180) \qquad \text{(C3b)}$$

The resulting mid-trophic production *F'n* which will be recruited by n-th mid-trophic population at each time step is derived from the solutions of (C1) as follows

$$F'_{nij} = S^m_{nij}, \quad m = \left[t_{r\,ij}\right]$$

### 5.4. Computing mid-trophic biomass

The transport of each mid-trophic component in the two horizontal dimensions x and y and the change of their biomass is described by the advection-diffusion-reaction equation:

$$\frac{\partial F_n}{\partial t} = D\left(\frac{\partial^2 F_n}{\partial x^2} + \frac{\partial^2 F_n}{\partial y^2}\right) - \frac{\partial}{\partial x}(\hat{u}F_n) - \frac{\partial}{\partial y}(\hat{v}F_n) - \lambda F_n + F_n' \qquad \text{(C4)}$$

where *λ* is the mortality coefficient, $F_n'$ is the production and $F_n$ is the biomass of the n-th mid-trophic component.

The partial derivatives of equation (C4) are approximated by second order finite differences with upwind differencing of advective terms as described in Sibert et al. (1999). Zero-flux boundary conditions, representing zero transport of the biomass across the bounds are chosen in order to set impermeability of the computational domain. The resulting algebraic problem is solved with

help of well-known alternate direction implicit (ADI) method, which is stable and always converging to the unique solution of the given equation.

Although the equations (C1) and (C4) are solved on rectangular grid, a correction factor is defined as 1/cos(lat) with latitude in radians and used to account for the change of grid cell sizes with higher latitudes.

## Appendix D. Time of development at maturity and ambient temperature

| *species* | *taxa* | *ambient T°C* | *age at maturity (d)* | *Reference* |
|---|---|---|---|---|
| *Illex illecebrosus* | Cephalopod | 12.6 | 365 | Wood and O'Dor, 2000 |
| *Loligo vulgaris* | Cephalopod | 14.0 | 245 | Wood and O'Dor, 2000 |
| *Loligo forbesi* | Cephalopod | 14.0 | 365 | Wood and O'Dor, 2000 |
| *Loligo opalescens* | Cephalopod | 16.0 | 184 | Wood and O'Dor, 2000 |
| *Ommastrephes bartramii* | Cephalopod | 23 | 310 | Ichii et al., 2004 |
| *Euprymna scolopes* | Cephalopod | 23.0 | 80 | Wood and O'Dor, 2000 |
| *Idiosepius pygmaeus* | Cephalopod | 25.2 | 50 | Wood and O'Dor, 2000 |
| *Sepioteuthis lessoniana* | Cephalopod | 26.2 | 150 | Forsythe et al., 2001, Jackson and Moltschaniwskyj, 2002 |
| *Sepioteuthis lessoniana* | Cephalopod | 27 | 110 | Forsythe et al., 2001 |
| *Tropical squids (Loliolus noctiluca, Loligo chinensis, Idiodepius pygmaeus)* | Cephalopod | 28 | 120 | Jackson and Choat, 1992 |
| *Sepiella inermis* | Cephalopod | 30.0 | 90 | Wood and O'Dor, 2000 |
| *Sepioteuthis lessoniana* | Cephalopod | 30.0 | 90 | Wood and O'Dor, 2000 |
| *Sepioteuthis lessoniana* | Cephalopod | 20.6 | 192 | Forsythe et al., 2001 |
| *Pandalus borealis* | Crustacean | 0 | 2009 | Hansen and Aschan 2000 |
| *Pandalus borealis* | Crustacean | 0 | 2191 | Hansen and Aschan 2000 |
| *Pandalus borealis* | Crustacean | 1 | 2557 | Hansen and Aschan 2000 |
| *Pandalus borealis* | Crustacean | 1.4 | 2191 | Hansen and Aschan 2000 |
| *Pandalus borealis* | Crustacean | 1.7 | 2009 | Hansen and Aschan 2000 |
| *Pandalus borealis* | Crustacean | 2.5 | 2557 | Hansen and Aschan 2000 |
| *Pandalus borealis* | Crustacean | 4 | 1826 | Hansen and Aschan 2000 |
| *Pandalus borealis* | Crustacean | 4.5 | 1095 | Hansen and Aschan 2000 |
| *Nycthiphanes simplex* | Crustacean | 24 | 60 | Siegel 2000 |
| *Euphausia superba* | Crustacean | 4 | 1095 | Siegel 2000 |
| *Euphausia eximia* | Crustacean | 18 | 210 | Siegel 2000 |
| *Euphausia pacifica* | Crustacean | 12 | 365 | Siegel 2000 |
| *Metherytrops microphtalma* | Crustacean | 2 | 912.5 | Ikeda 1992 |
| *Thysanopoda tricuspidata, T. monocantha, T. aequalis, Nematoscelis tenella, Euphausia diomedae* | Crustacean | 17 | 300 | Roger 1971 |
| *Mallotus villosus* | Fish | 4 | 1095 | Carscadden et al., 1997 |
| *leuroglossus schmidti* | Fish | 5 | 730 | Abookire et al., 2002 |
| *Stenobrachius leucopsarus* | Fish | 5 | 1460 | Abookire et al., 2002 |
| *Clupea harrengus* | Fish | 8 | 1095 | Reid et al. 1999 |
| *Clupea harrengus* | Fish | 5 | 1278 | Alheit and Hagen 1997; Corten 1999 |
| *Engraulis ringens* | Fish | 14 | 450 | Schwartzlose et al. 1999 |

| *species* | *taxa* | *ambient T°C* | *age at maturity (d)* | *Reference* |
|---|---|---|---|---|
| *Engraulis japonicus* | Fish | 16 | 300 | Takahashi and Watanabe 2004 |
| *Engraulis mordax* | Fish | 15 | 365 | Schwartzlose et al. 1999 |
| *Engraulis capensis* | Fish | 13 | 360 | Schwartzlose et al. 1999 |
| *Engraulis encrasicolus* | Fish | 10 | 400 | Samsun et al. 2004 |
| *Engraulis encrasicolus* | Fish | 13 | 365 | Allain, 2005 |
| *Sardinops melanostictus* | Fish | 12 | 700 | Hunter and Wada, 1993 |
| *Sardinops sagax* | Fish | 14 | 730 | Schwartzlose et al. 1999 |
| *Encrasicholina punctifer* | Fish | 30 | 120 | Dalzell 1993 |
| *Vinciguerria Nimbarria* | Fish | 28 | 120 | Stéquert et al. 2003 |
| *Scomber japonicus* | Fish | 12 | 730 | Prager and Mc Call 1988 |
| *Clupea pallasi* | Fish | 7 | 1095 | Hunter and Wada, 1993 |

## Figures (all figures are original and to be printed in BW and colour online)

**Figure 1**

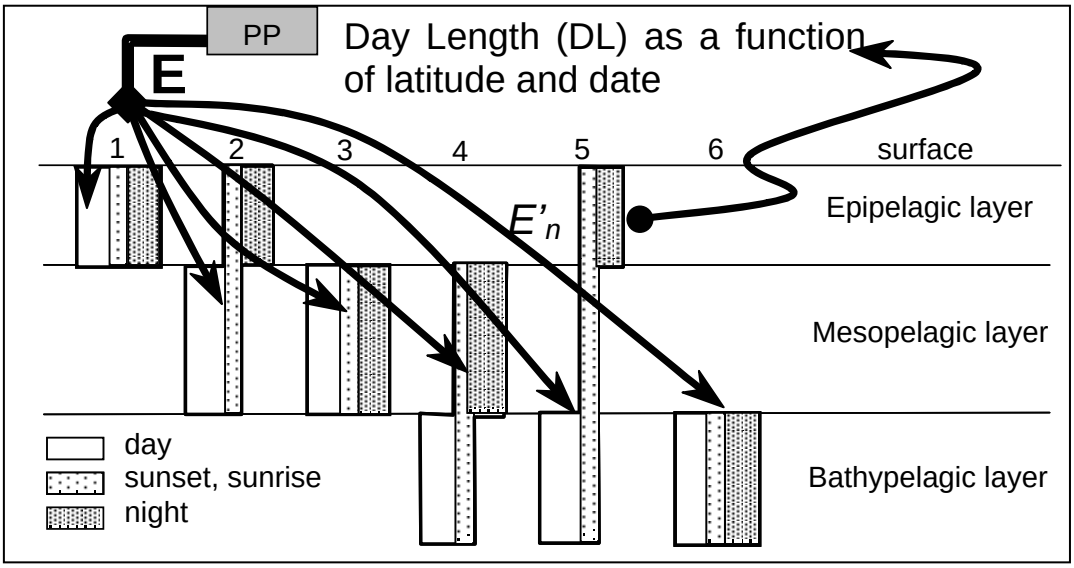


Figure 1 Conceptual model of the mid-trophic components in the pelagic ecosystem. Daily vertical distribution patterns of the micronekton in the pelagic ecosystem: 1, epipelagic; 2, migrant mesopelagic; 3, non-migrant mesopelagic; 4, migrant bathy-pelagic; 5, highly-migrant bathypelagic; 6, non-migrant bathypelagic. The part of energy (*E*) transferred from primary production (PP) to intermediate trophic levels is redistributed ($E_n'$) through the different components.

**Figure 2**

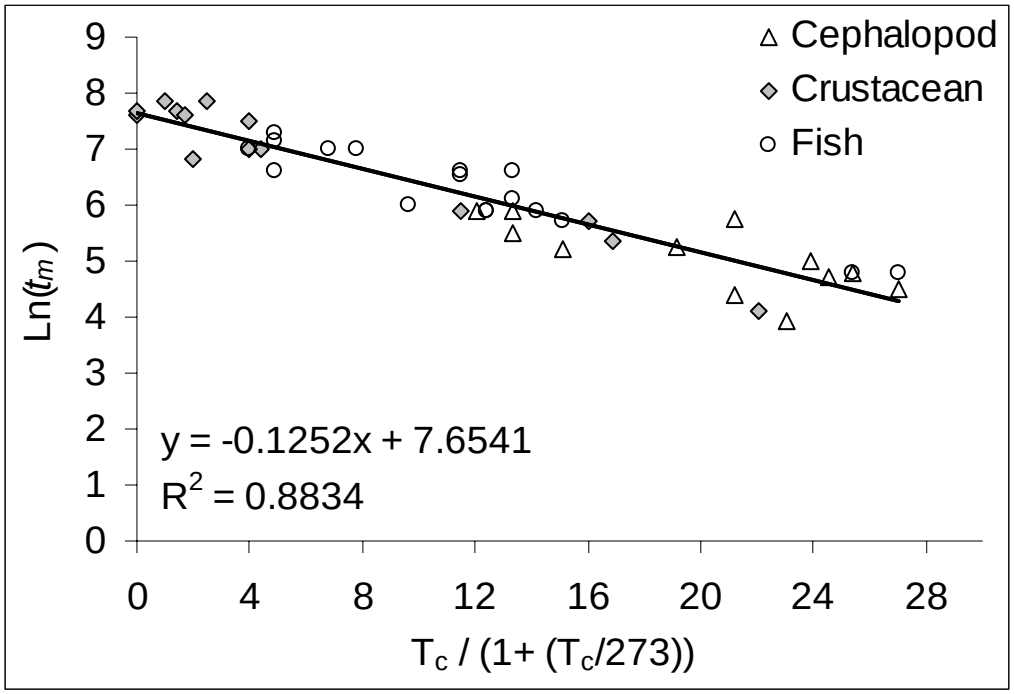


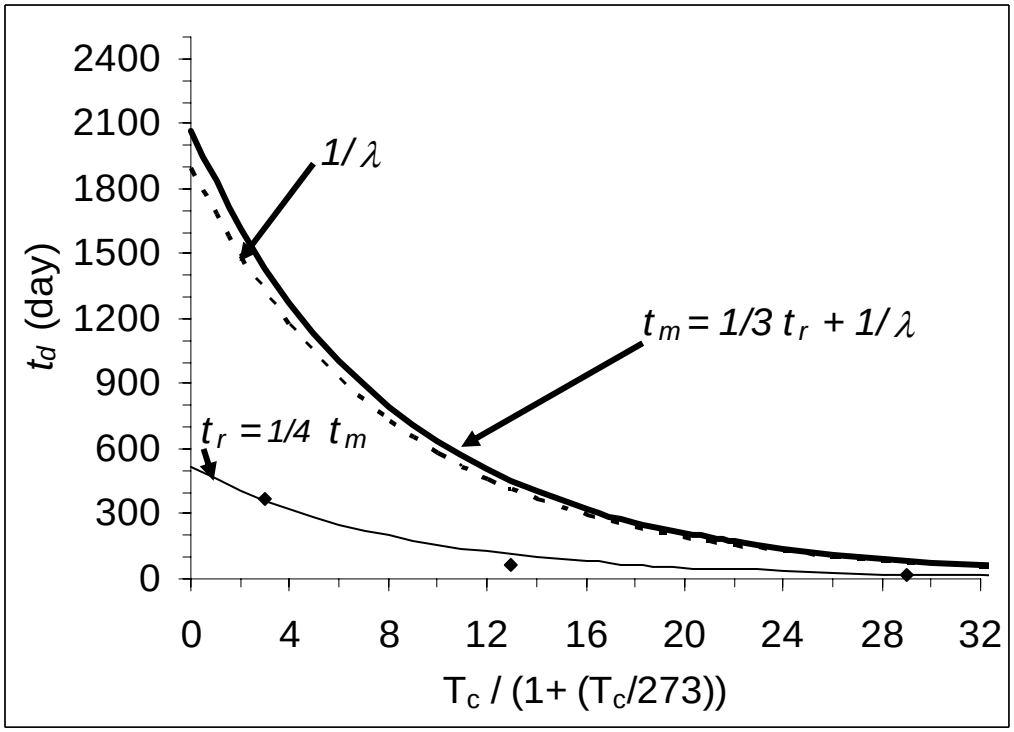


Figure 2 Age at maturity of species ($t_m$) in relation to their average habitat temperature (ambient temperature $T_c$). Observations derived from the literature are used to estimate the

coefficients of the exponential decreasing functions predicting the turn-over of mid-trophic groups (see text for explanation). Coefficients are estimated from a log-linear regression. For each Class of species, observations are sorted by decreasing average habitat temperature.

**Cephalopods:** *Bathypolypus arcticus*[1], *Octopus doeini*[1], *Illex illecebrosus*[1], *Loligo vulgaris*[1], *Loligo forbesi*[1], *Loligo opalescens*[1], *Sepioteuthis lessoniana*[1], *Ommastrephes bartramii*[4], , *Euprymna scolopes*[1], *Idiosepius pygmaeus*[1], *Sepioteuthis lessoniana*[2], *Sepioteuthis lessoniana*[3], *Loliolus noctiluca*[5], *Loligo chinensis*[5], *Idiodepius pygmaeus*[5], *Sepiella inermis*[1], *Sepioteuthis lessoniana*[1]. **Crustaceans:** *Pandalus borealis*[6], *Pandalus borealis*[6], *Pandalus borealis*[6], *Pandalus borealis*[6], *Pandalus borealis*[6], *Metherytrops microphtalma*[7], *Pandalus borealis*[6], *Pandalus borealis*[6], *Euphausia superba*[8], *Pandalus borealis*[6], *Euphausia pacifica*[8], *Thysanopoda tricuspidata*[9], *T. monocantha*[9], *T. aequalis*[9], *Nematoscelis tenella*[9], *Euphausia diomedae*[9], *Euphausia eximia*[8], *Nycthiphanes simplex*[8]. **Fish:** *Mallotus villosus*[10], *Leuroglossus schmidti*[11], *Stenobrachius leucopsarus*[11], *Clupea harrengus*[12], *Clupea pallasi*[13], *Clupea harrengus*[14], *Engraulis encrasicolus*[15], *Sardinops melanostictus*[16], *Scomber japonicus*[17], *Engraulis capensis*[18], *Engraulis encrasicolus*[19], *Engraulis ringens*[18], *Sardinops sagax*[18], *Engraulis mordax*[18], *Engraulis japonicus*[20], *Vinciguerria Nimbarria*[21], *Encrasicholina punctifer*[22].

References: [1]Wood and O'Dor (2000); [2]Jackson and Moltschaniwskyj (2002); [3]Forsythe et al. (2001); [4]Ichii et al. (2004); [5]Jackson and Choat (1992); [6]Hansen and Aschan (2000); [7]Ikeda (1992); [8]Siegel (2000); [9]Roger (1971); [10]Carscadden et al. (1997); [11]Abookire et al. (2002); [12]Alheit and Hagen (1997); [13]Hunter and Wada (1993); [14]Reid et al. (1999); [15]Samsun et al. (2004); [16]Hunter and Wada (1993); [17]Prager and Mc Call (1988); [18]Schwartzlose et al. (1999); [19]Allain G. (2005); [20]Takahashi and Watanabe (2004); [21]Stéquert et al. (2003); [22]Dalzell (1993).

**Figure 3**

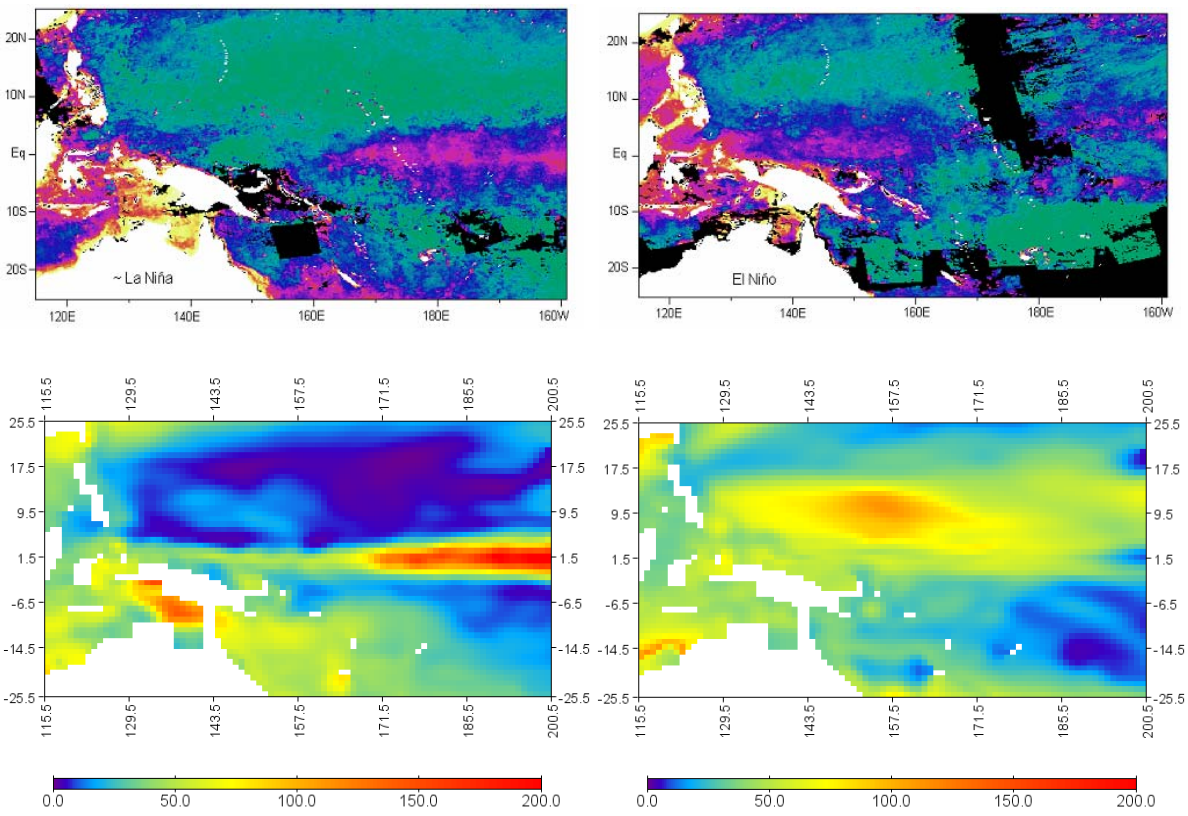


Figure 3 Comparison between observed (top) chlorophyll concentration (CZCS satellite) and predicted primary production (ESSIC NPZD model, mmol C $m^{-2}$ $d^{-1}$) during La Niña and El Niño phases in the western equatorial Pacific (Sept. 1981 and Dec. 1982 respectively).

**Figure 4**

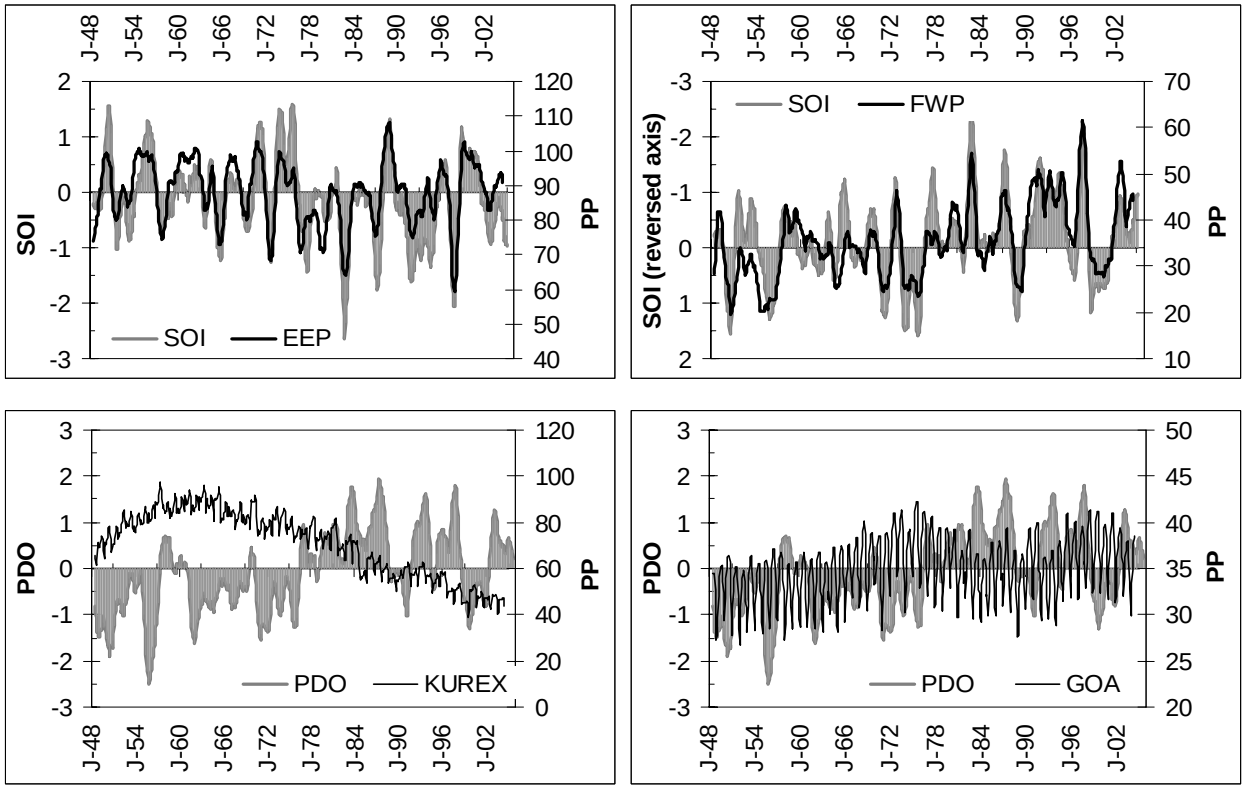


Figure 4 Predicted time series of average total primary production (black curves, in mmol $C \cdot m^{-2} \cdot d^{-1}$) in four different geographical boxes superimposed over the southern Oscillation or the Pacific Decadal oscillation indices (SOI and PDO respectively, grey shaded curves). **EEP**: Eastern equatorial Pacific, 10°N-10°S; 140°W-100°W. **FWP**: Far Western Pacific, 15°N-5°S; 125°E-160°E. **KUREX**: Kuroshio Extension, 40°N-30°N; 140°E-170°E. **GOA**: Gulf of Alaska, 62°N-50°N;160°W-130°W.

**Figure 5**

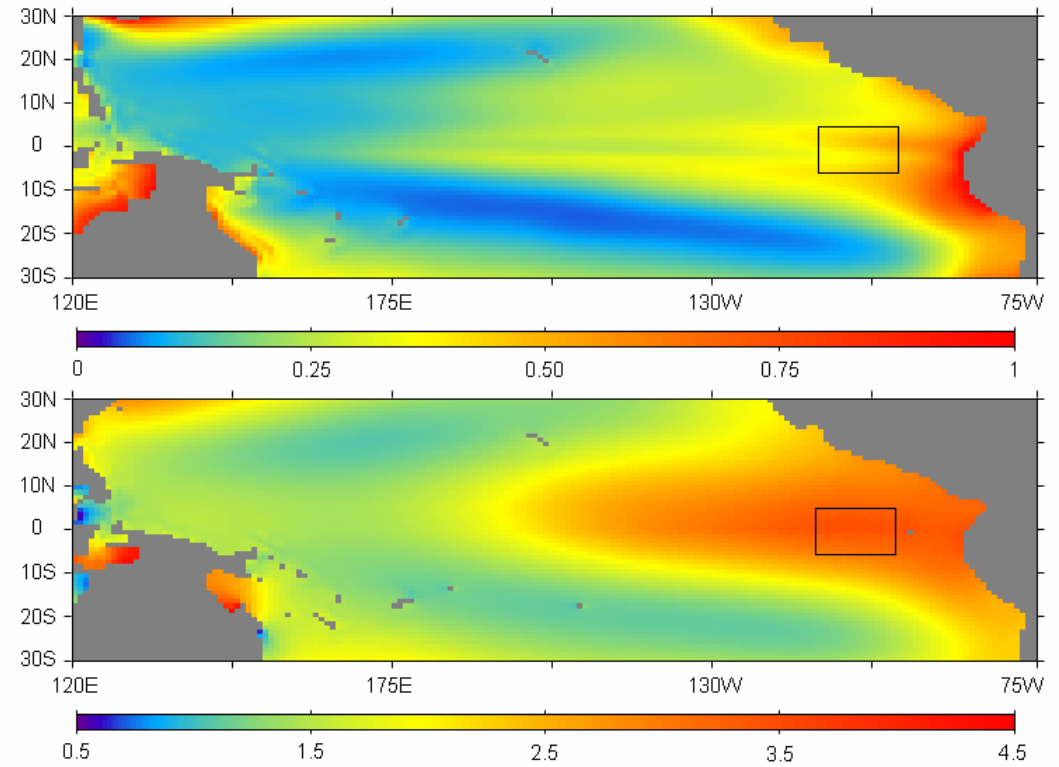
30N
20N
10N
0
10S
20S
30S
120E
175E
130W
75W
0
0.25
0.50
0.75
1
0.5
1.5
2.5
3.5
4.5

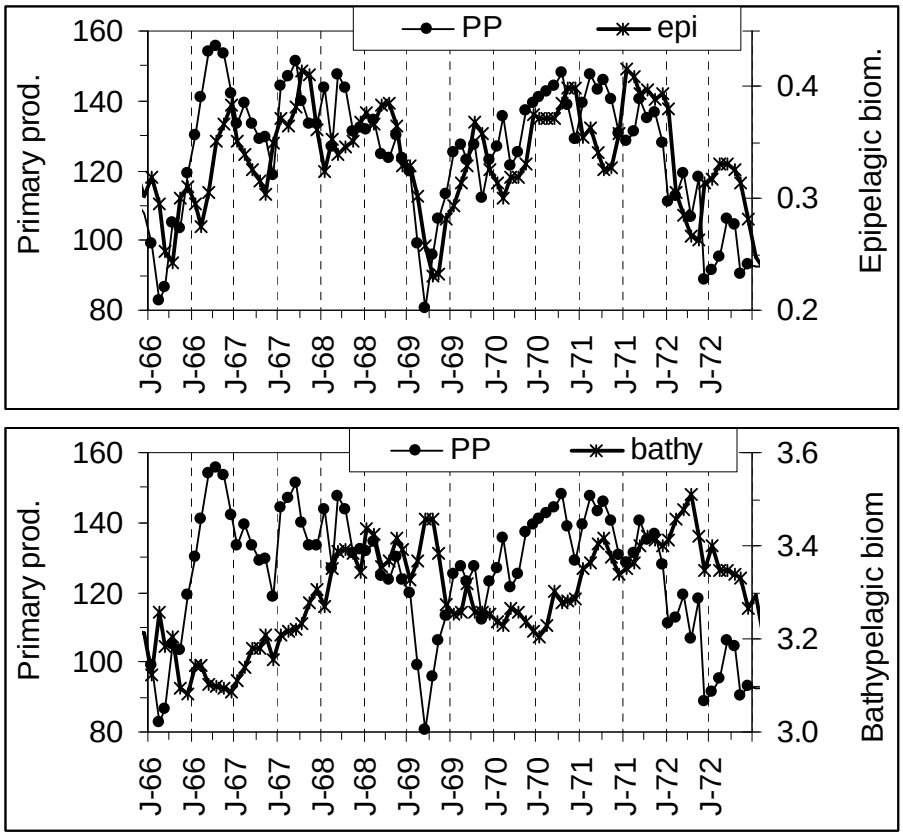
PP
epi
bathy
Primary prod.
Epipelagic biom.
Bathypelagic biom
160
140
120
100
80
0.4
0.3
0.2
3.6
3.4
3.2
3.0
J-66
J-67
J-68
J-69
J-70
J-71
J-72

Figure 5 Average spatial distribution over all the time series (1948-2004) of purely epipelagic (a) and bathypelagic (b) groups. Due to difference in the habitat temperatures, turnover rates of mid-trophic populations are different. The average biomass time series of epipelagic (c) and bathypelagic (d) components for the box 5N-5S; 120W-100W (identified on the maps) indicate a lag with primary production of about 2 months for epipelagic group and 12-14 months for bathypelagic group. Primary production is in mmol C $m^{-2}$ $d^{-1}$ and biomass unit for mid-trophic groups in gWW $m^{-2}$.

**Figure 6**

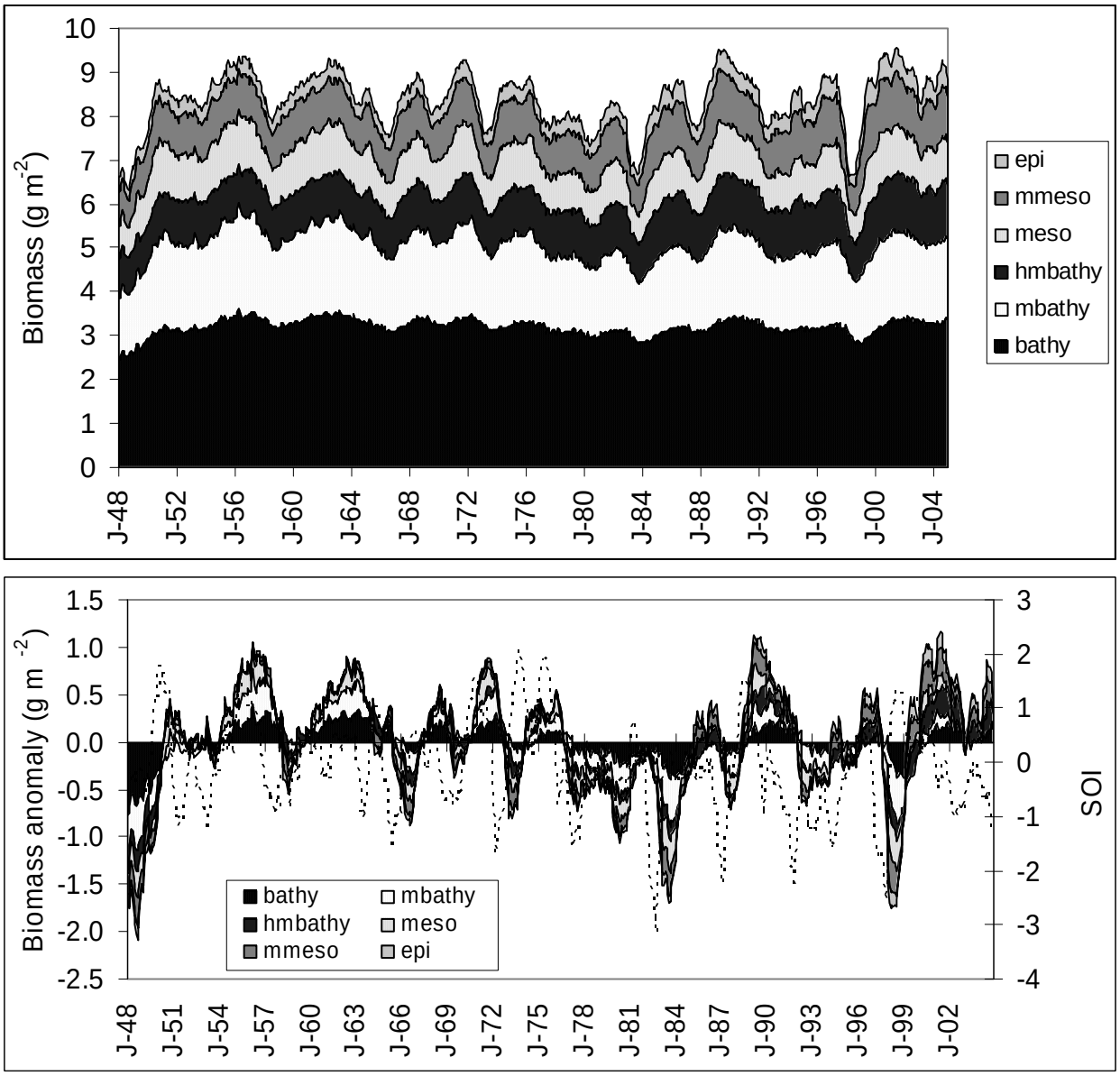


Figure 6 Time series of total biomass (in gWW $m^{-2}$) and anomaly in biomass (difference to the average of the time series) for the 6 mid-trophic functional groups predicted in the box 5N-5S; 120W-100W (c.f. map in Fig. 5). Southern Oscillation Index (SOI) is superimposed (dotted line) on the anomaly time series.

**Figure 7**

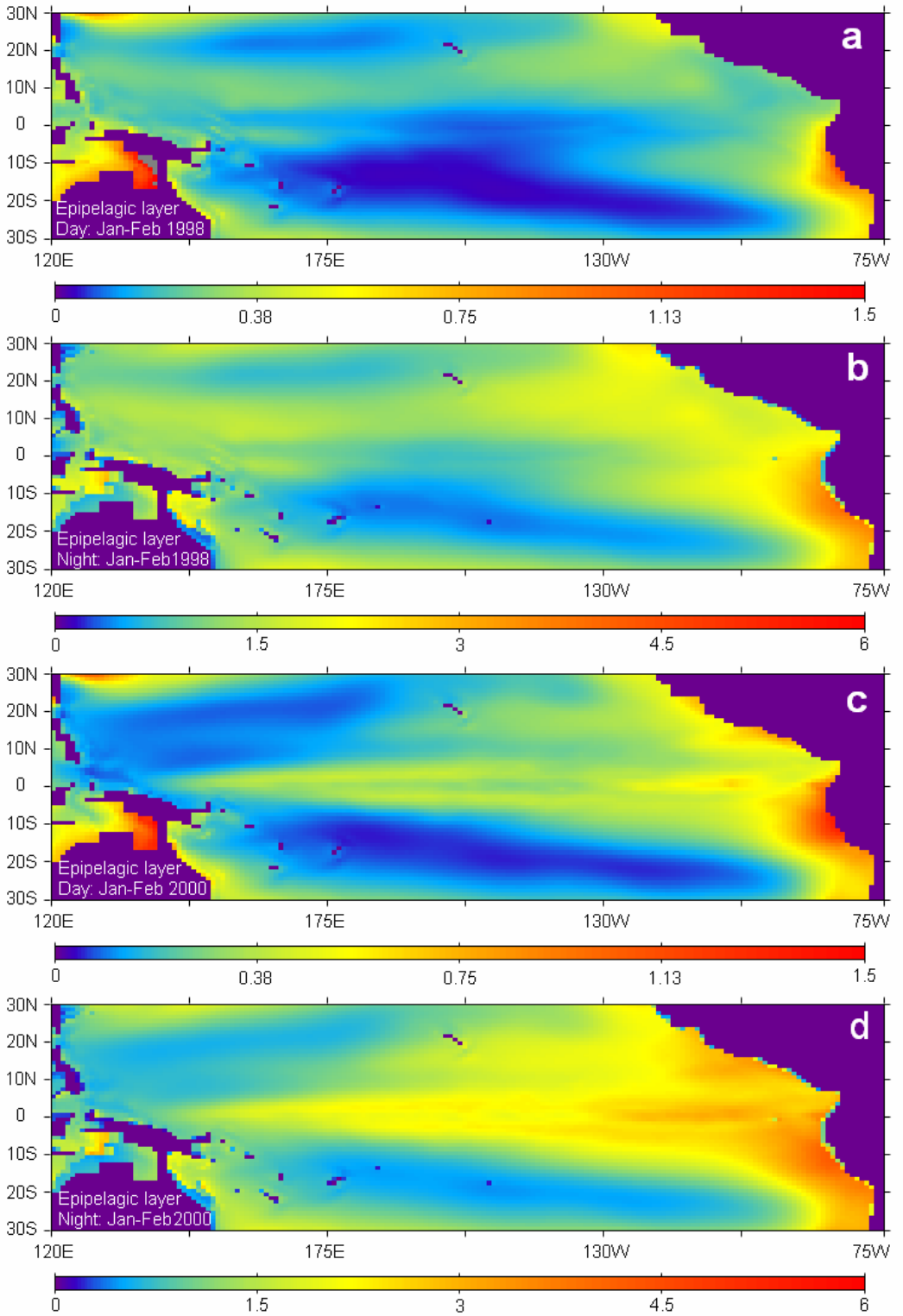


Figure 7 Interannual variability of micronekton biomass in the epipelagic layer (0-100 m) during day and night. The ENSO impact is shown with the distribution of forage biomass (in g

WW·m$^{-2}$) during Jan-Feb 1998 in the final stage of the 1997-98 El Niño event and at the end of the following La Niña event in Jan-Feb 2000.

**Figure 8**

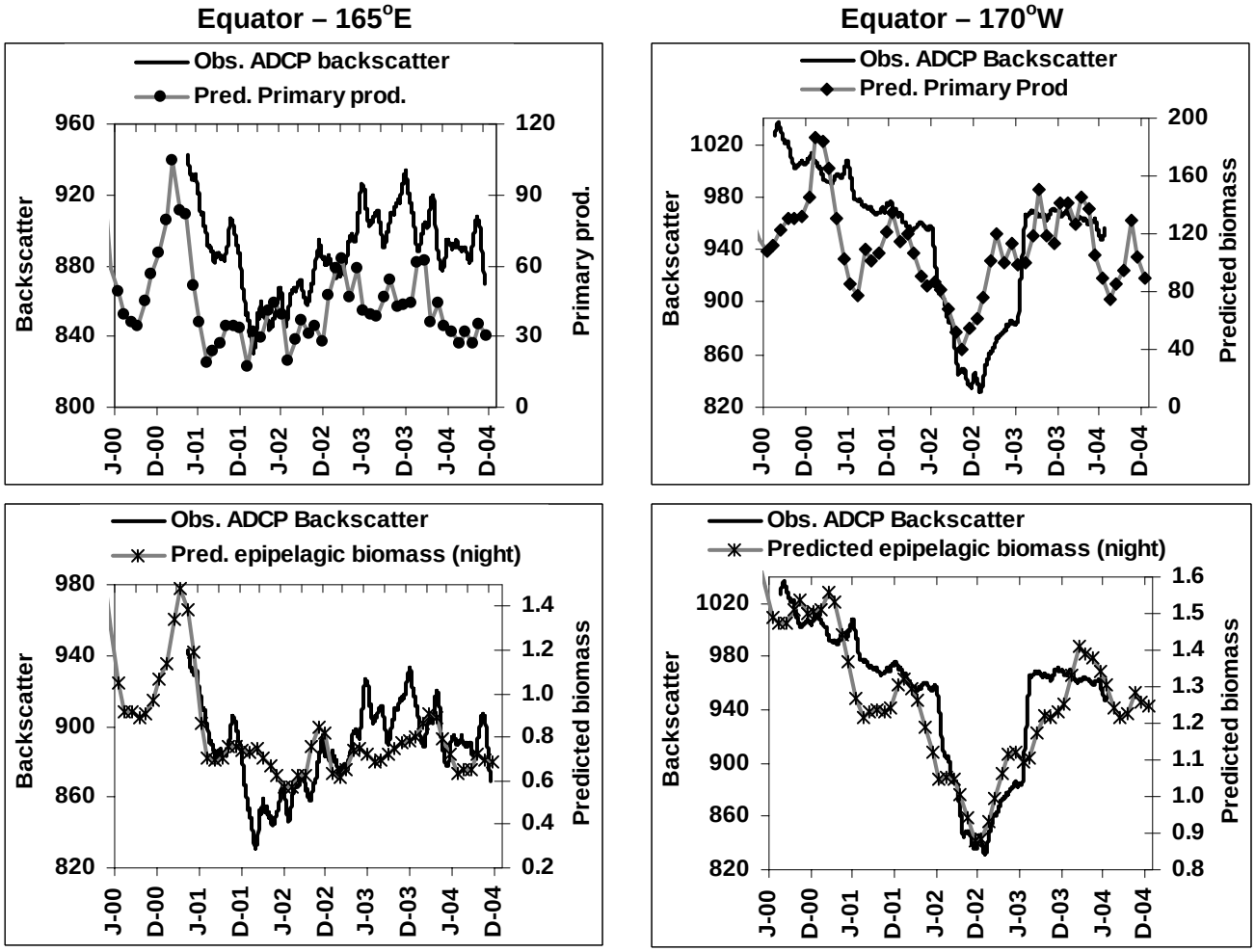


Figure 8 Comparison of the average time-series of ADCP backscatter intensity data at night of the TAO moorings on the Equator at 165°E and 170°W with model predicted primary production (mmol C $m^{-2}$ $day^{-1}$) and biomass of mid-trophic components present in the epipelagic layer at night (g $m^{-2}$). ADCP data kindly provided by Patricia Plimpton and Michael McPhaden of NOAA/PMEL (Plimpton et al., 2004). Data from the different deployments have been ajusted without formal calibration but instrumental difference observed from one deployment to the next one were low (max ~5 dB) comparatively to the natural variability (M.H. Radenac, pers. comm.).